Second SoWMEX/TiMREX Science Workshop
October 20, 2009 at Taipei, Taiwan

Development of a three-dimensional detection algorithm for precipitation cells in East Asia during the Meiyu/Baiu period

Taro Shinoda, Yusuke Fukamachi,

Hiroshi Uyeda, and Kazuhisa Tsuboki

(Hydrospheric Atmospheric Research Center, Nagoya University, Japan)

Stages of Precipitation Cells

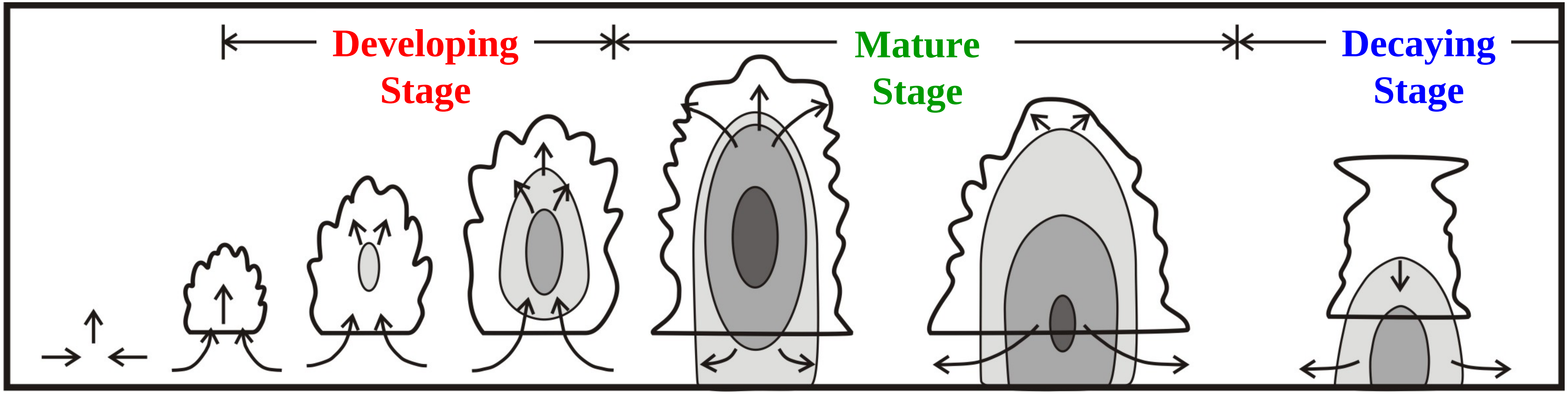

Purdom (1995) modified

Developing Stage : occupied by only updraft region
Mature Stage : occupied by both updraft and downdraft regions
Decaying Stage : occupied by only downdraft region

●Motivation

It is useful to detect the stages of precipitation cells automatically using dual-Doppler analyses:

for understanding the structure of precipitation systems,
for predicting a sudden heavy rainfall event.

Stages of Precipitation Cells

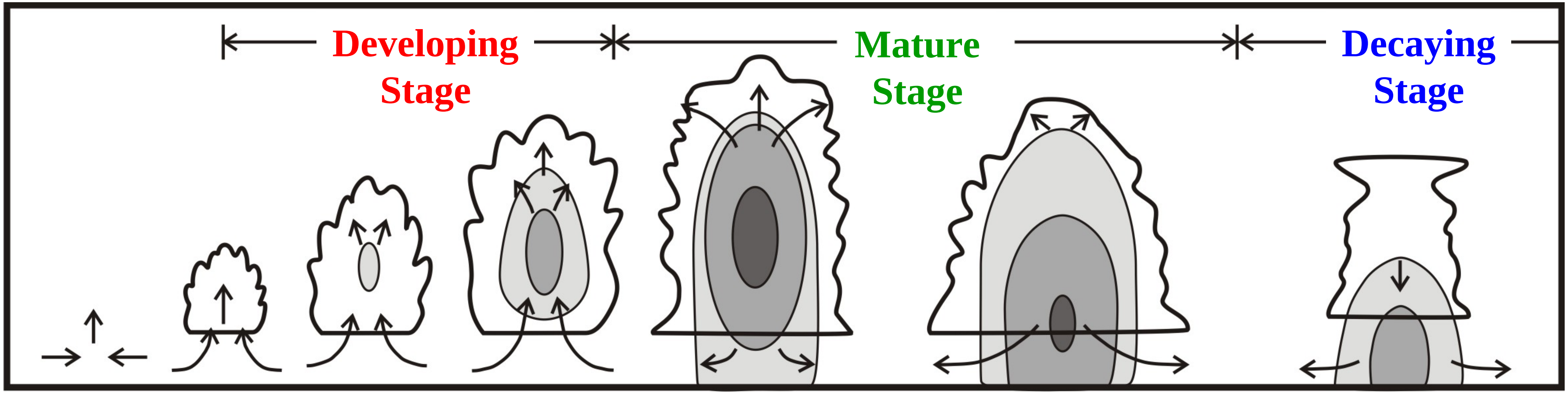

Purdom (1995) modified

Developing Stage : occupied by **only updraft region**

Mature Stage : occupied by **both updraft and downdraft regions**

Decaying Stage : occupied by **only downdraft region**

Purpose of this study is

to develop **a three-dimensional detection algorithm for precipitation cells** using **reflectivity** and **wind field** data calculated from dual-Doppler analyses.

Doppler Radar Data

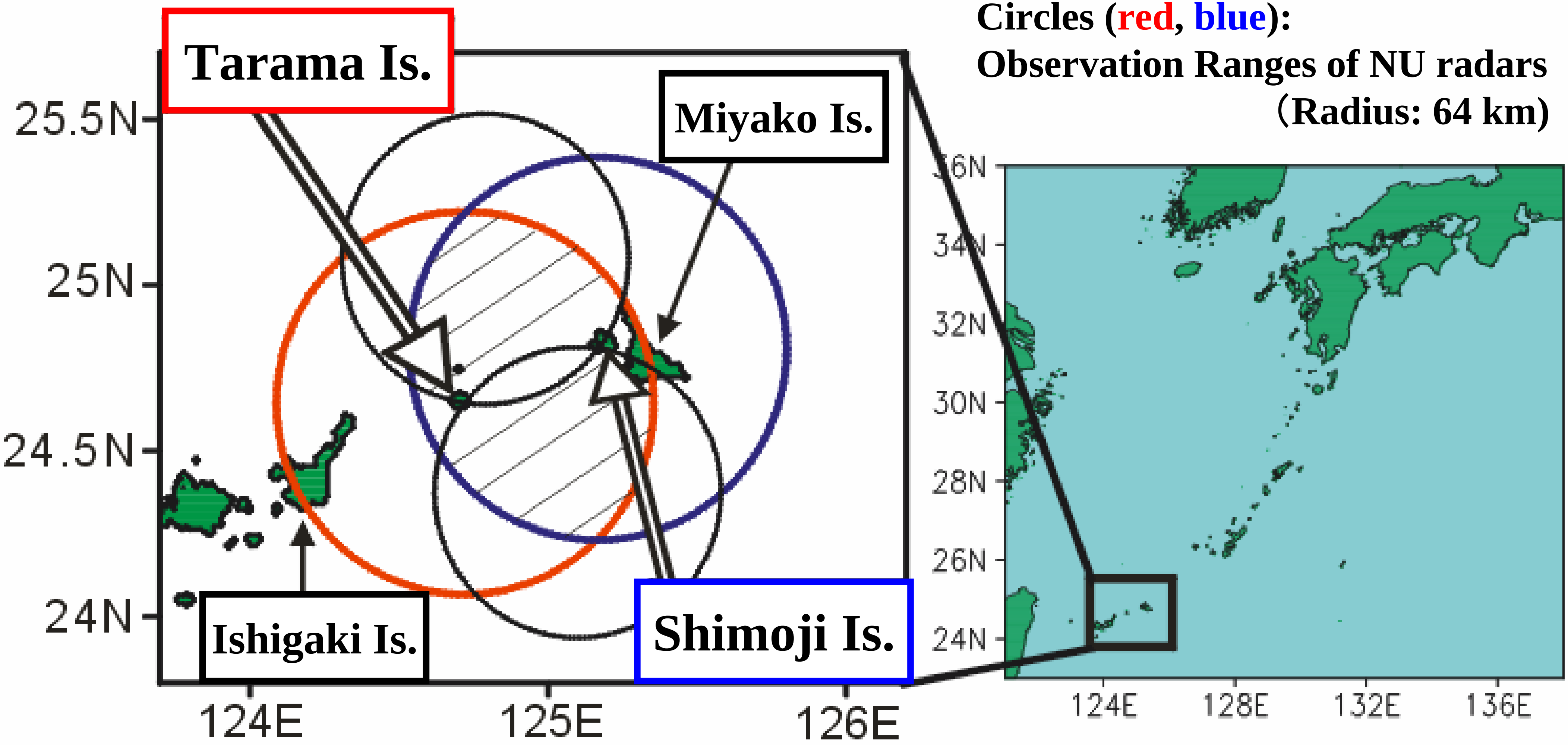

Circles (red, blue):
Observation Ranges of NU radars
(Radius: 64 km)

- We have conducted a dual-Doppler observation around Miyako Island during the Baiu period in 2006.
- Radars were situated at Tarama and Shimoji Islands.
- We examined dual-Doppler analyses shown in Gao (1999) and calculated three-dimensional wind fields.

Doppler Radar Data

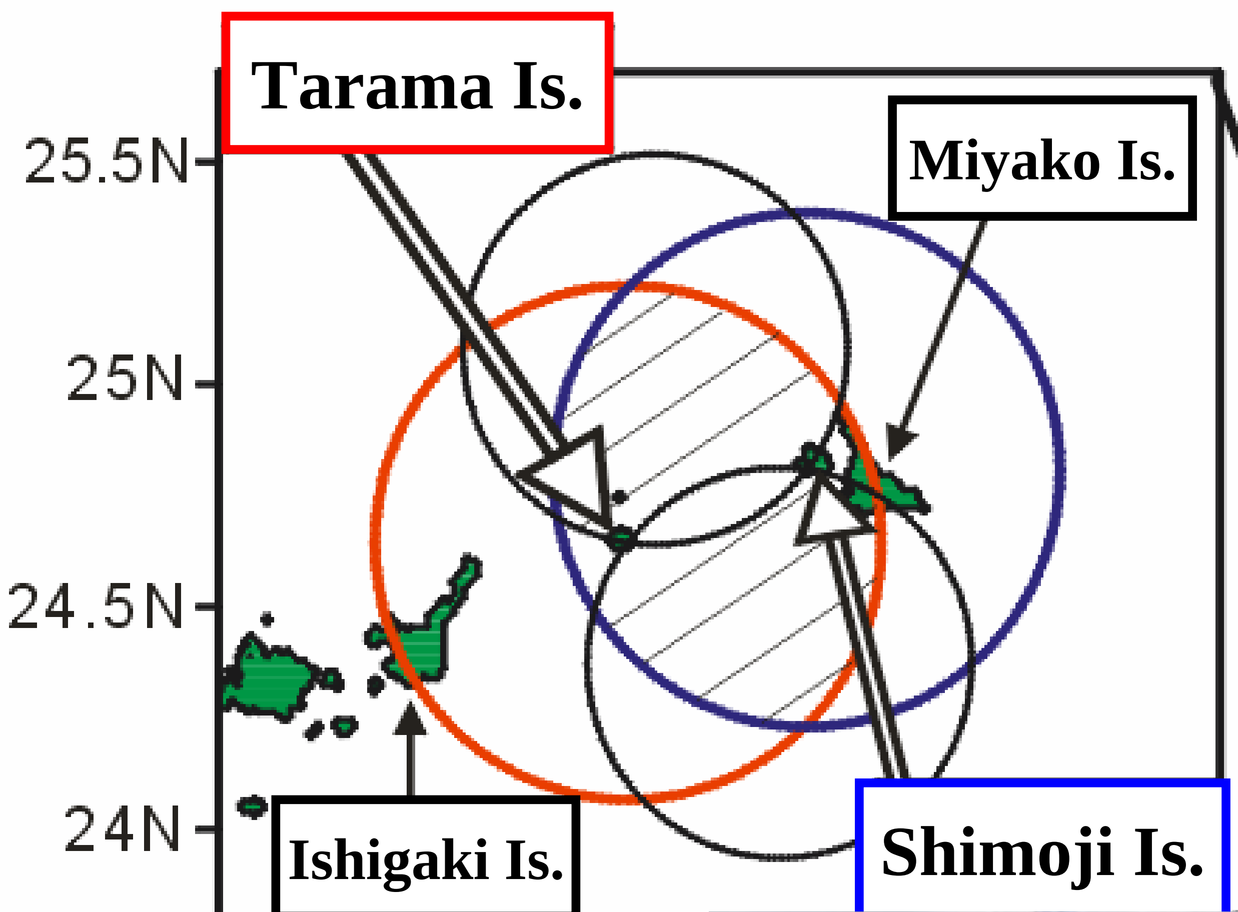

Circles (red, blue):
Observation Ranges of NU radars
(Radius: 64 km)

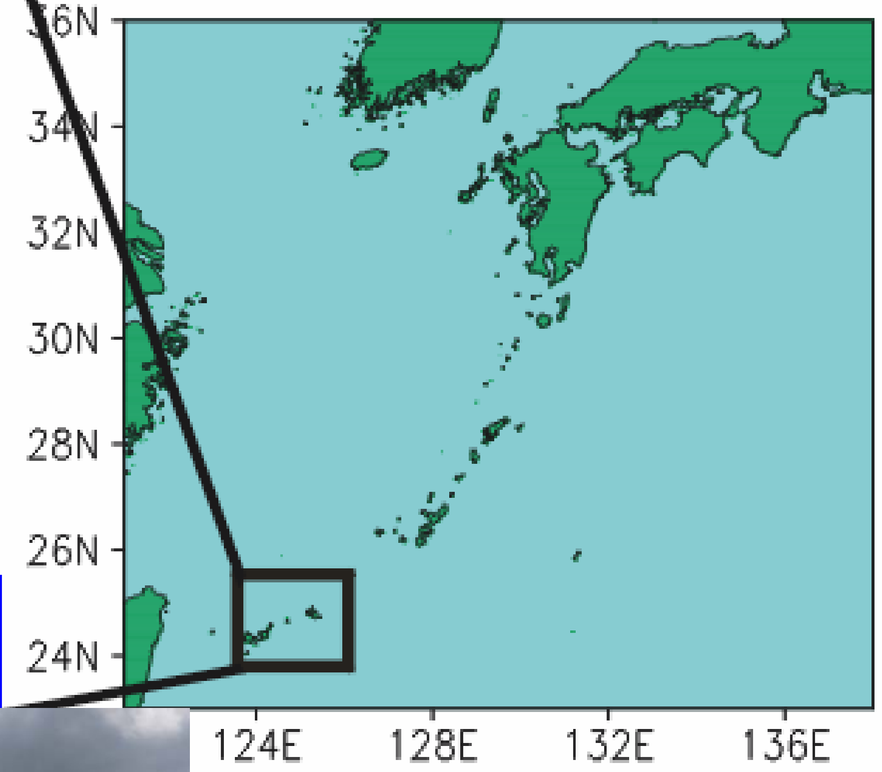

The three-dimensional detection algorithm for precipitation cells (1/4)

Reflectivity data in 3-dimensional Cartesian coordinate

↓

Remove stratiform regions using the BBF method; Pick up convective regions (over 30 dBZe)

↓

The central parts of cells are recognized in each layer: negative regions of 2nd derivative for reflectivity

↓

connecting the central parts of cells vertically

↓

three-dimensional region of each cell is fixed

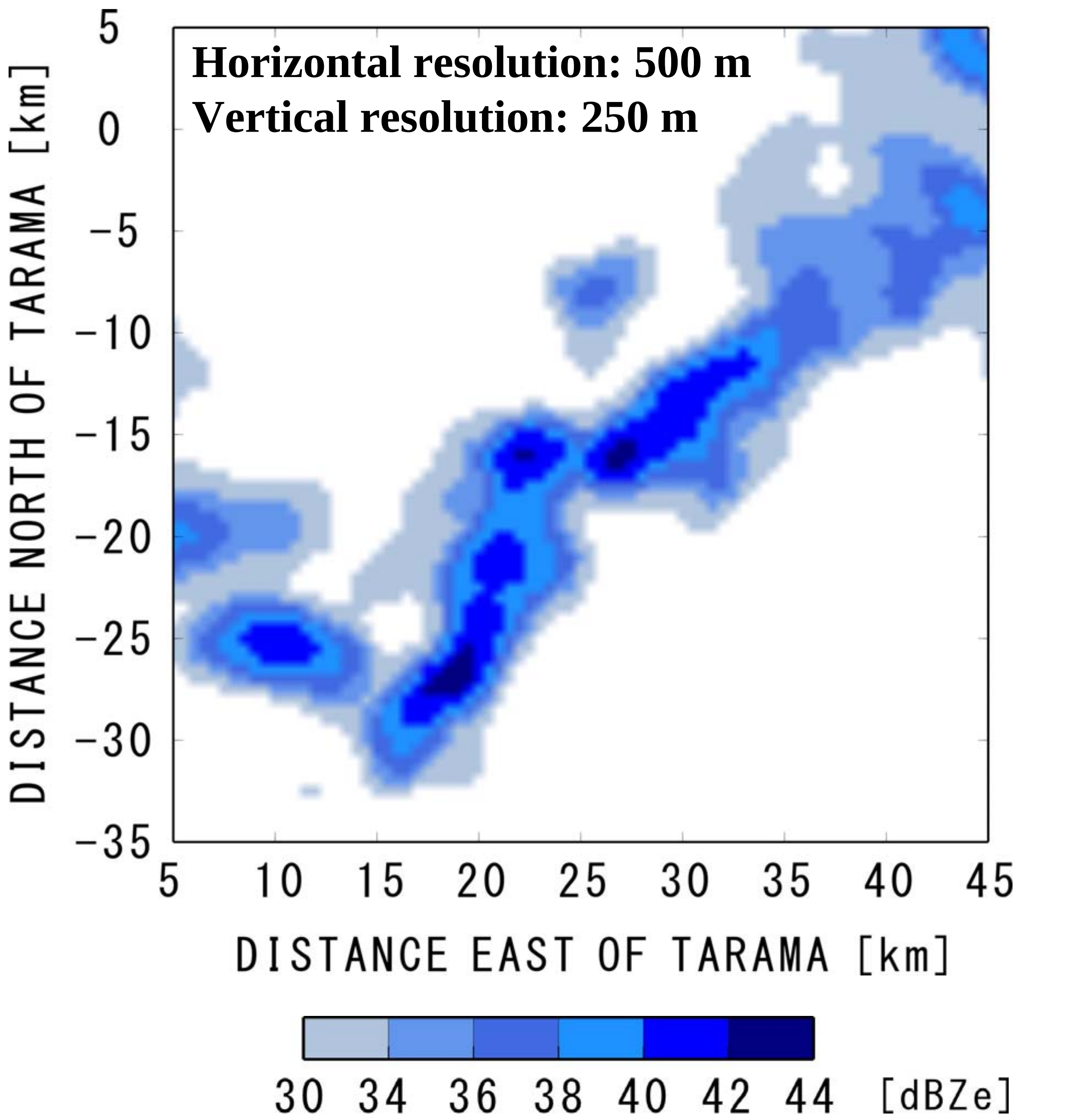

The three-dimensional detection algorithm for precipitation cells (2/4)

Reflectivity data in 3-dimensional Cartesian coordinate

↓

Remove stratiform regions using the BBF method; Pick up convective regions (over 30 dBZe)

↓

The central parts of cells are recognized in each layer: negative regions of 2nd derivative for reflectivity

↓

connecting the central parts of cells vertically

↓

three-dimensional region of each cell is fixed

The second derivatives are calculated along four directions (E-W, N-S, NE-SW, and NW-SE).

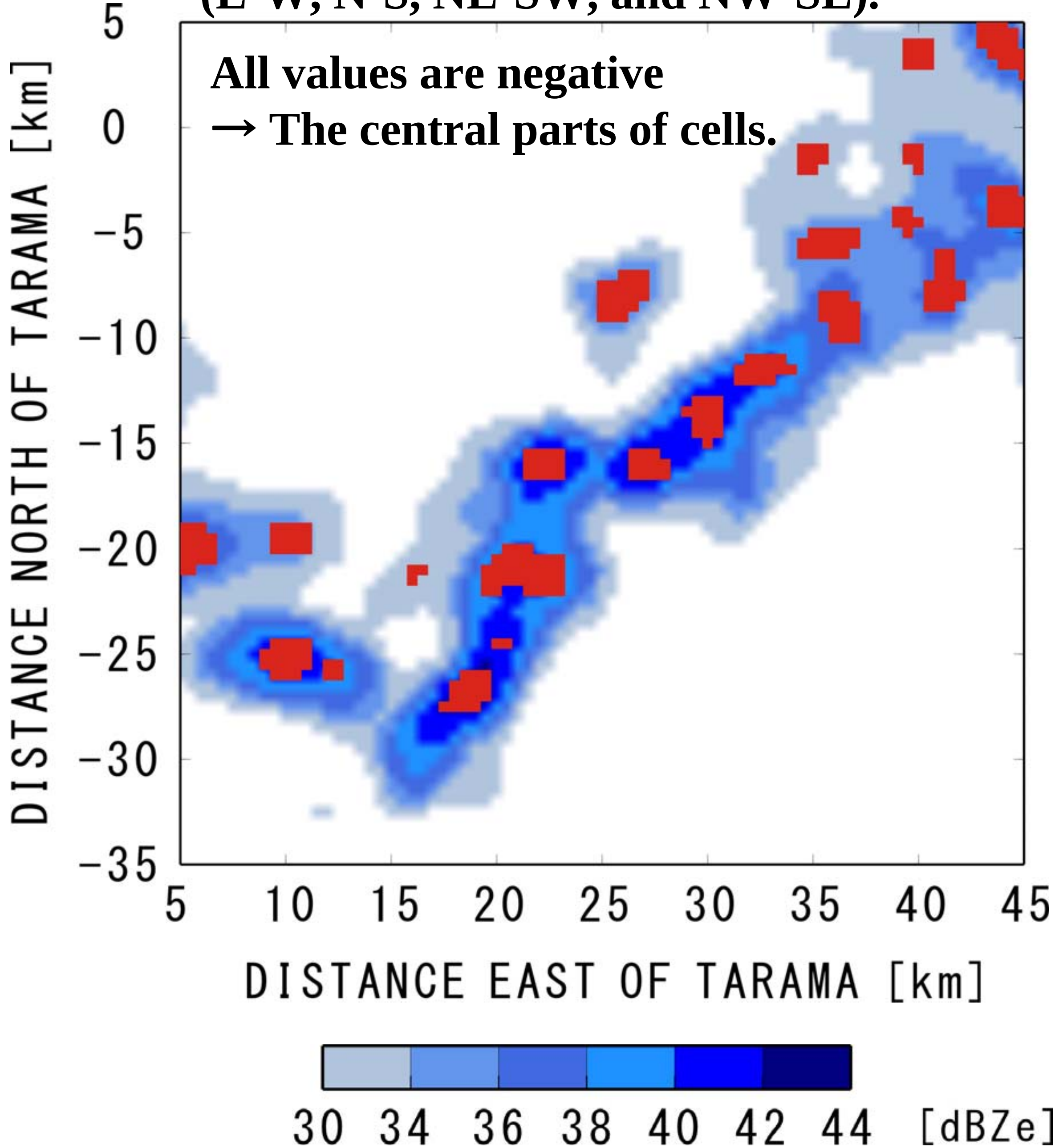

Detecting Central Parts of Precipitation Cells

We calculate the second derivative for 3-dimensional reflectivity along four directions at each level. (W-E, S-N, SW-NE, NW-SE)

$$\frac{\partial f(r)}{\partial r} = \frac{2}{(dr)^2}\left[\frac{f(r+\delta r)+f(r-\delta r)}{2} - f(r)\right]$$

Maximum reflectivity regions correspond to negative ones of the second derivative for Ref.
→ We recognize these regions as the central parts of cells.

Sample of a reflectivity distribution

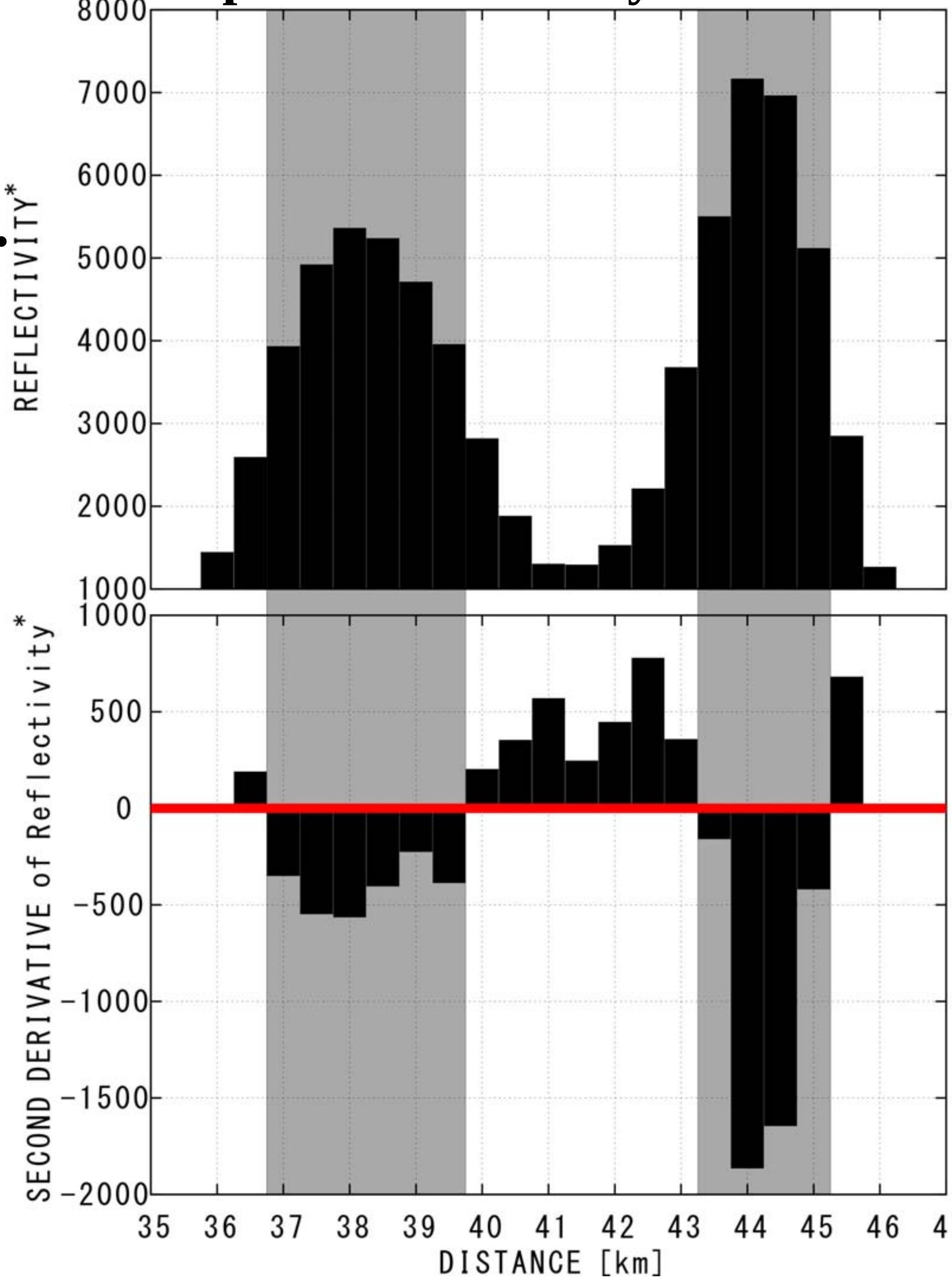

The three-dimensional detection algorithm for precipitation cells (2/4)

Reflectivity data in 3-dimensional Cartesian coordinate

↓

Remove stratiform regions using the BBF method; Pick up convective regions (over 30 dBZe)

↓

The central parts of cells are recognized in each layer: negative regions of 2nd derivative for reflectivity

↓

connecting the central parts of cells vertically

↓

three-dimensional region of each cell is fixed

The second derivatives are calculated along four directions (E-W, N-S, NE-SW, and NW-SE).

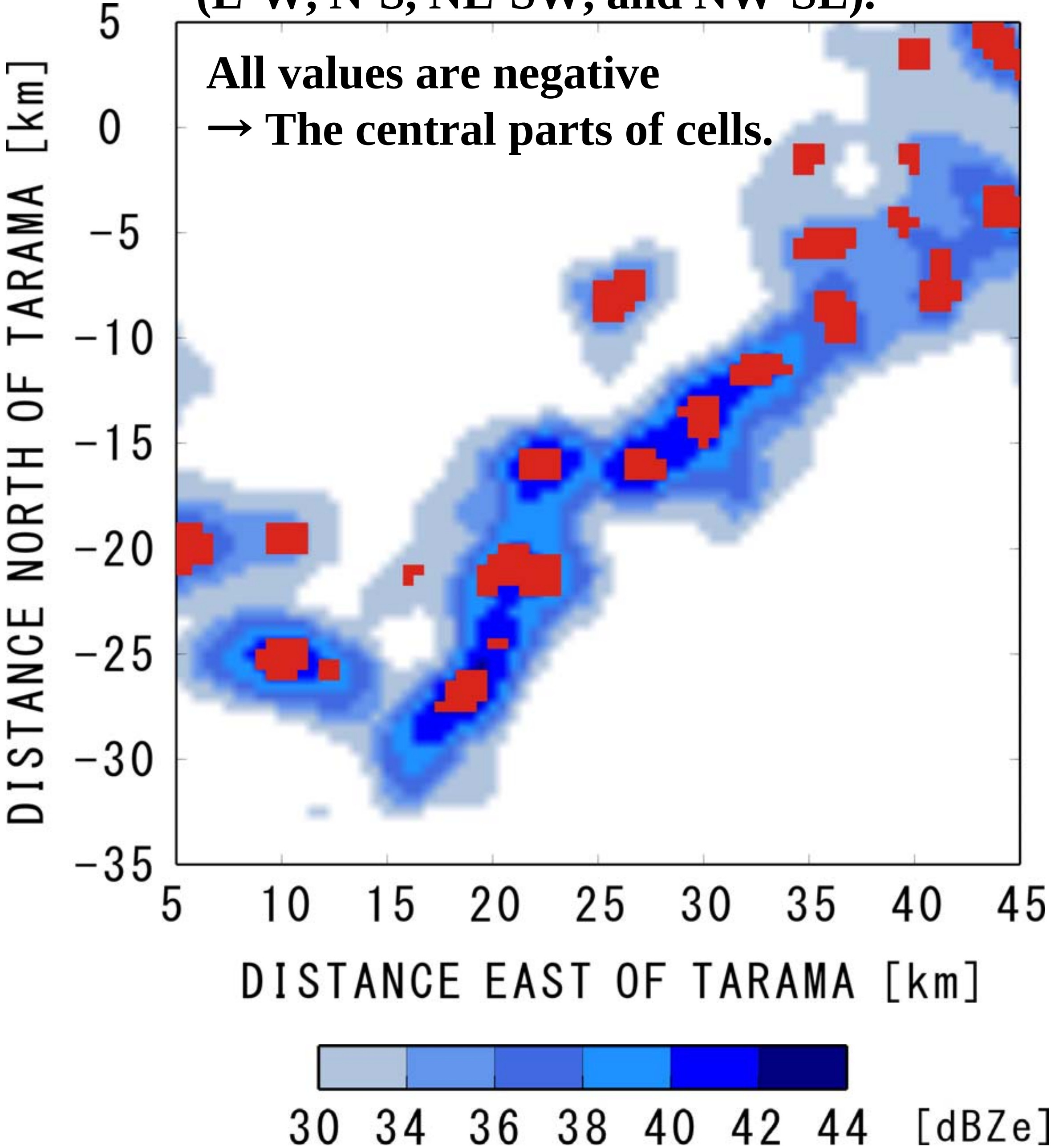

The three-dimensional detection algorithm for precipitation cells (3/4)

Reflectivity data in 3-dimensional Cartesian coordinate

↓

Remove stratiform regions using the BBF method; Pick up convective regions (over 30 dBZe)

↓

The central parts of cells are recognized in each layer: negative regions of 2nd derivative for reflectivity

↓

connecting the central parts of cells vertically

↓

three-dimensional region of each cell is fixed

Using the Connected Component Labeling (CCL: A method of image processing)

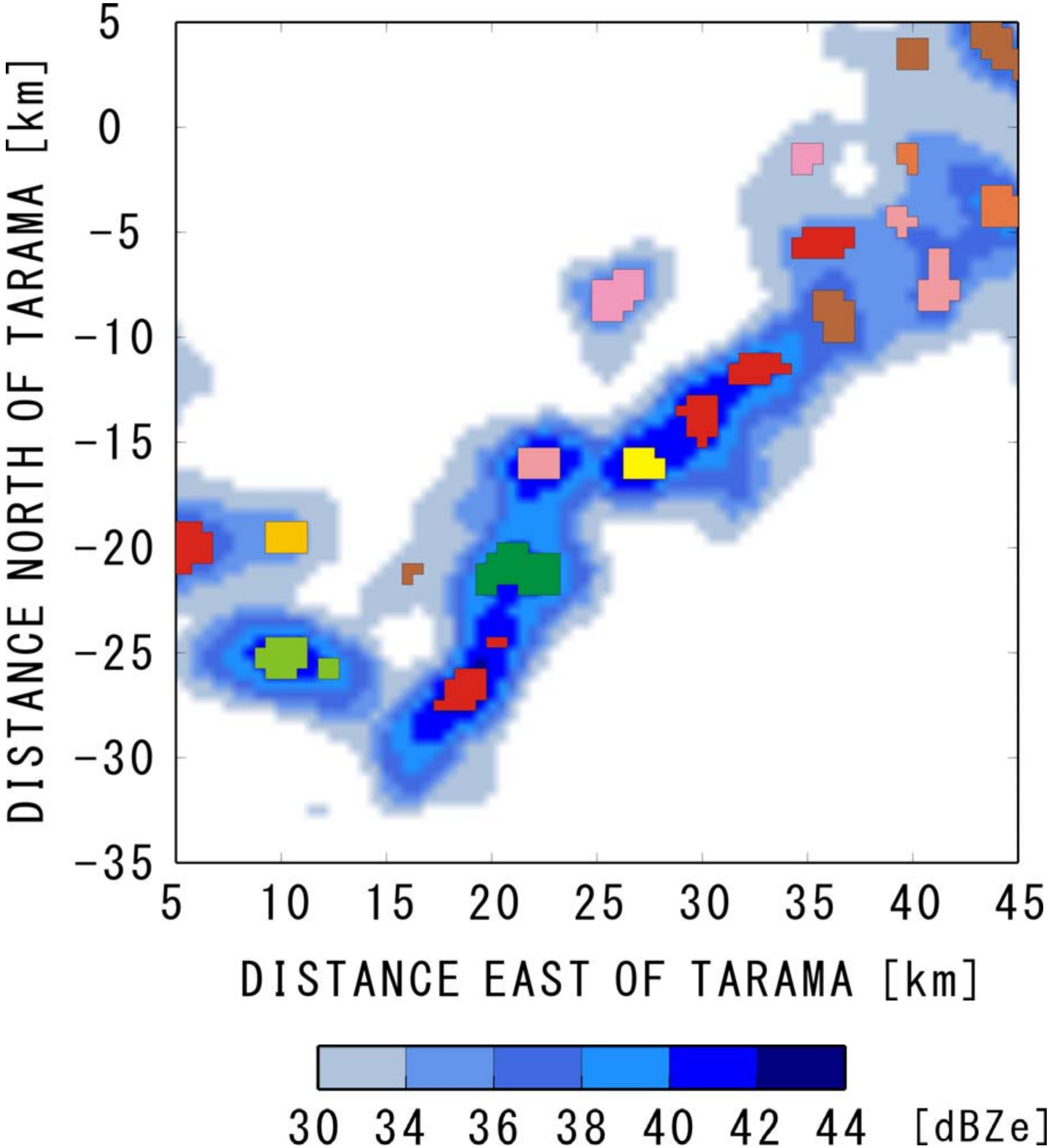

An Outline of the Connected Component Labeling (Suematsu, 2000, in Japanese)

This method is used in the image processing engineering.

First scanning

Conducting three-dimensional scanning,
Search labeled grids and numbering (gray grids)

Exist neighboring labeled grids?
(Search 26 grids)

- No numbers → Set new label
- Only a kind of numbers → Set same label of neighboring grids
- More than two numbers → Set minimum number of labels

Second scanning

Change the number of labels

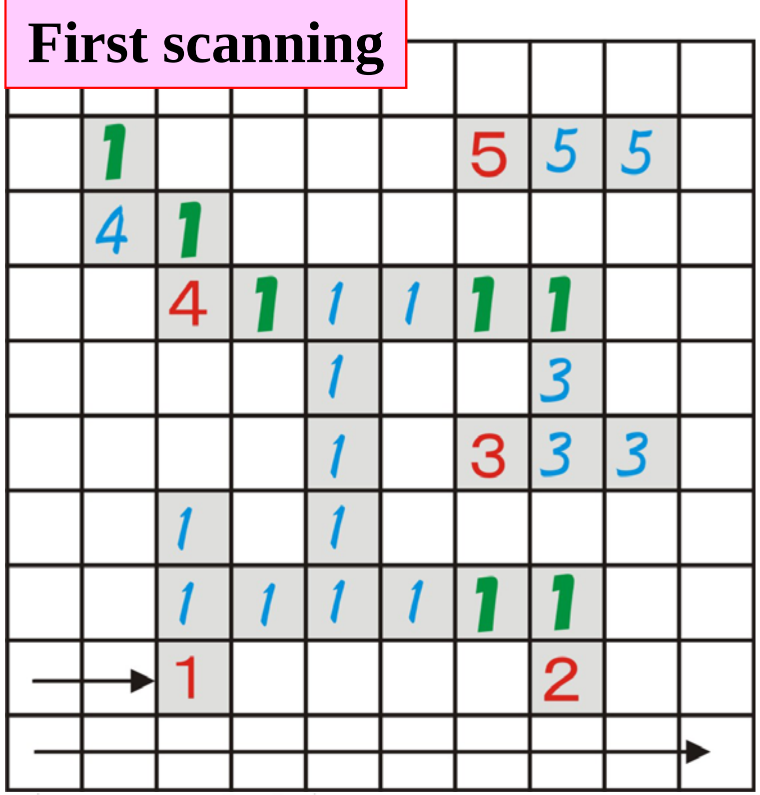

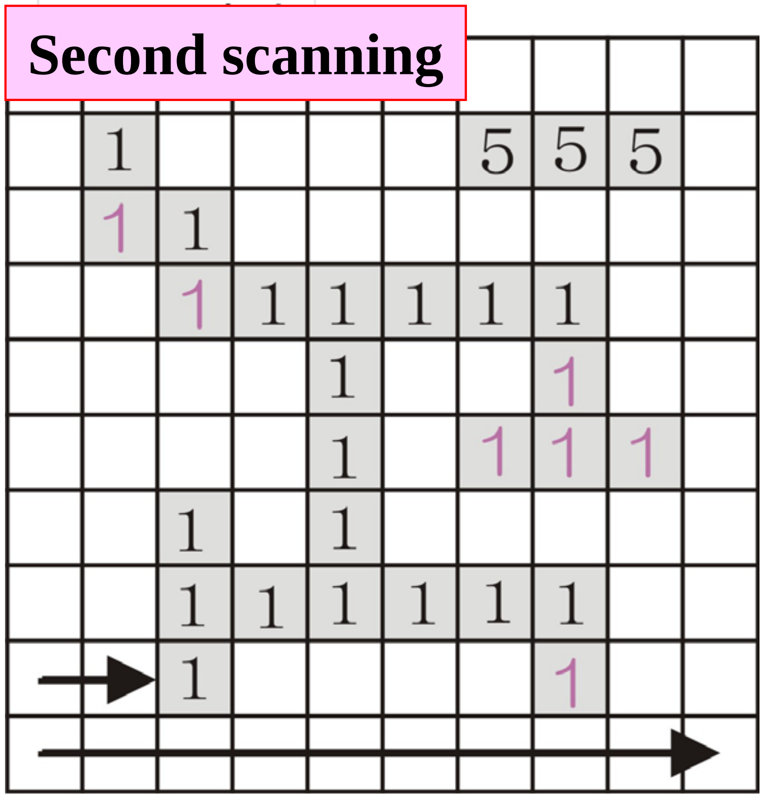

The three-dimensional detection algorithm for precipitation cells (3/4)

Reflectivity data in 3-dimensional Cartesian coordinate

↓

Remove stratiform regions using the BBF method; Pick up convective regions (over 30 dBZe)

↓

The central parts of cells are recognized in each layer: negative regions of 2nd derivative for reflectivity

↓

connecting the central parts of cells vertically

↓

three-dimensional region of each cell is fixed

Using the Connected Component Labeling (CCL: A method of image processing)

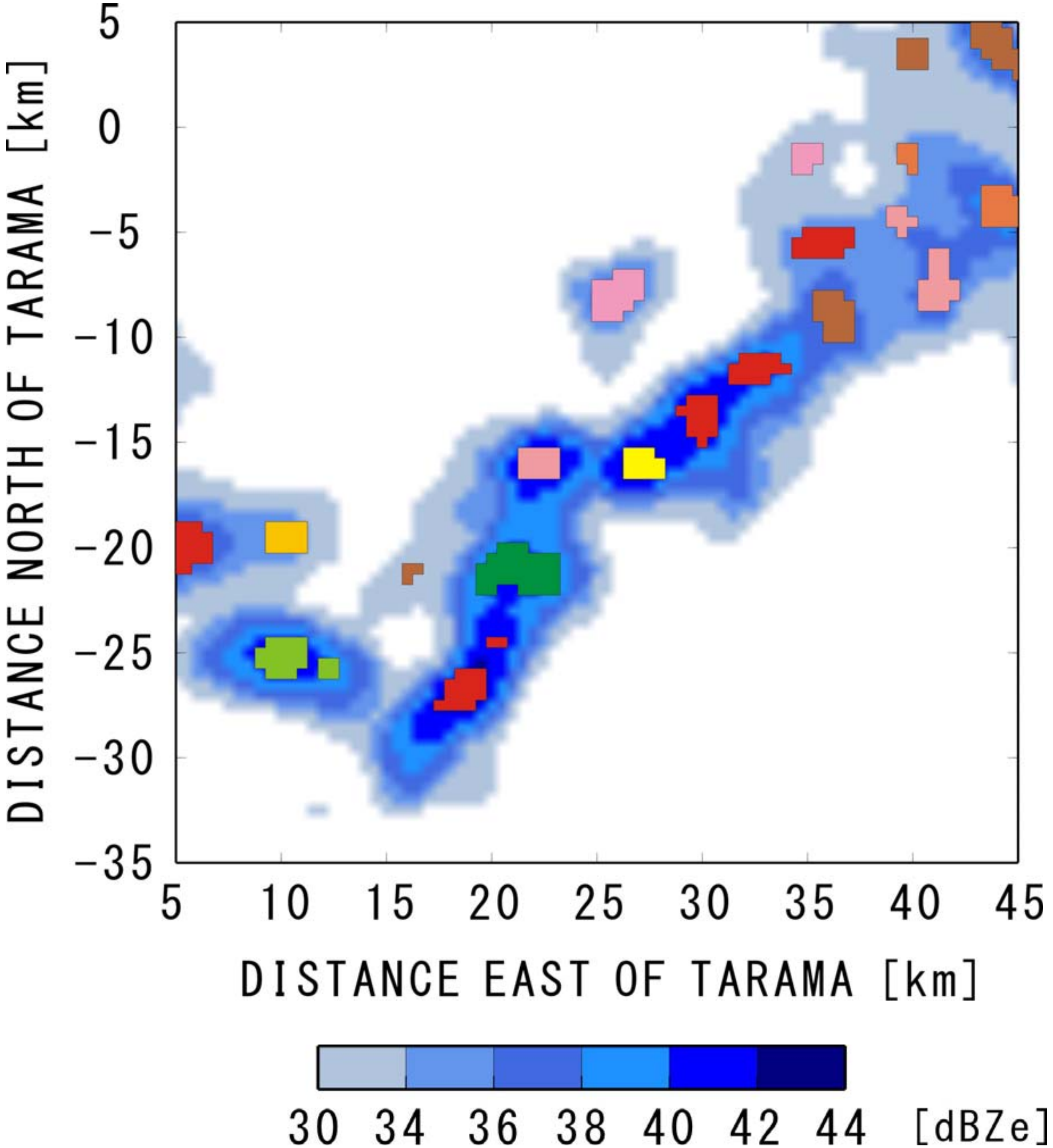

The three-dimensional detection algorithm for precipitation cells (4/4)

Reflectivity data in 3-dimensional Cartesian coordinate

↓

Remove stratiform regions using the BBF method; Pick up convective regions (over 30 dBZe)

↓

The central parts of cells are recognized in each layer: negative regions of 2nd derivative for reflectivity

↓

connecting the central parts of cells vertically

↓

three-dimensional region of each cell is fixed

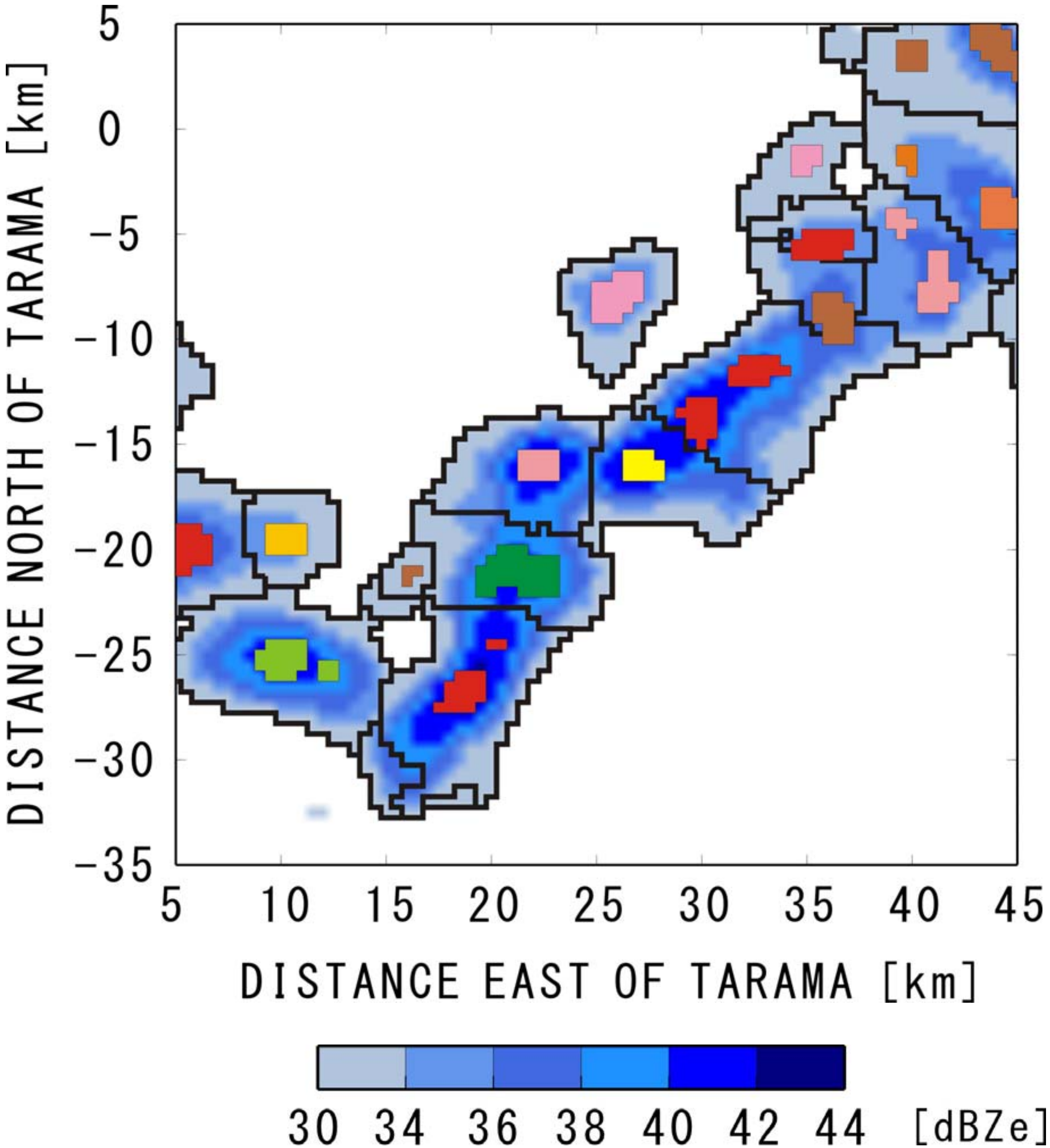

Sample of Detecting Precipitation Cells

Vertical cross-section along 1-2.

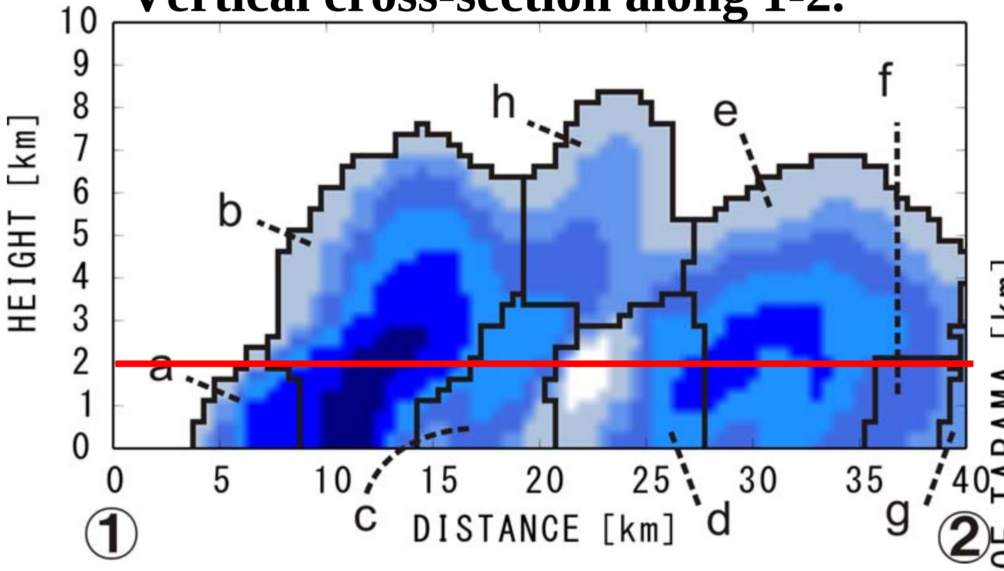

Vertical cross-section along 3-4.

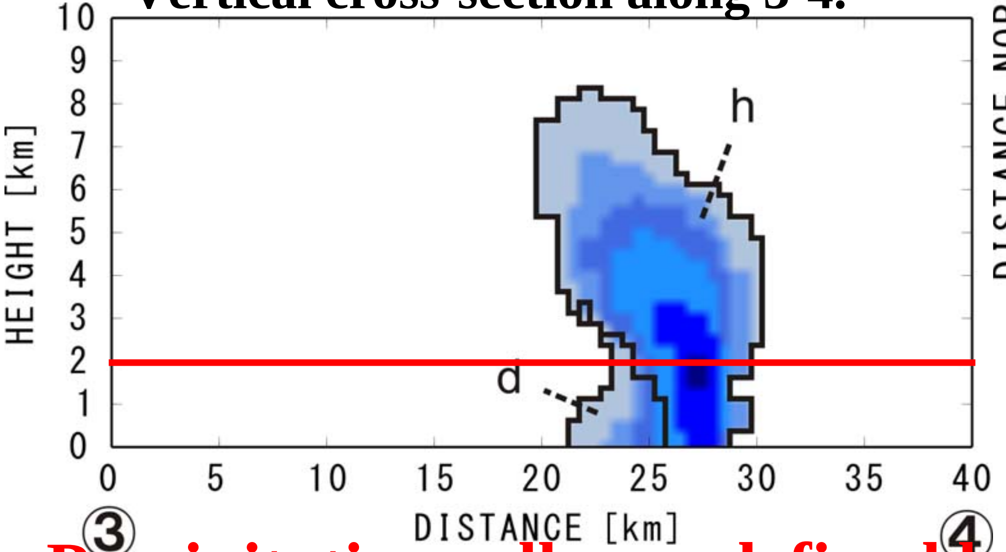

Reflectivity at a height of 2 km
by Tarama radar at 0700 LST on June 09, 2006

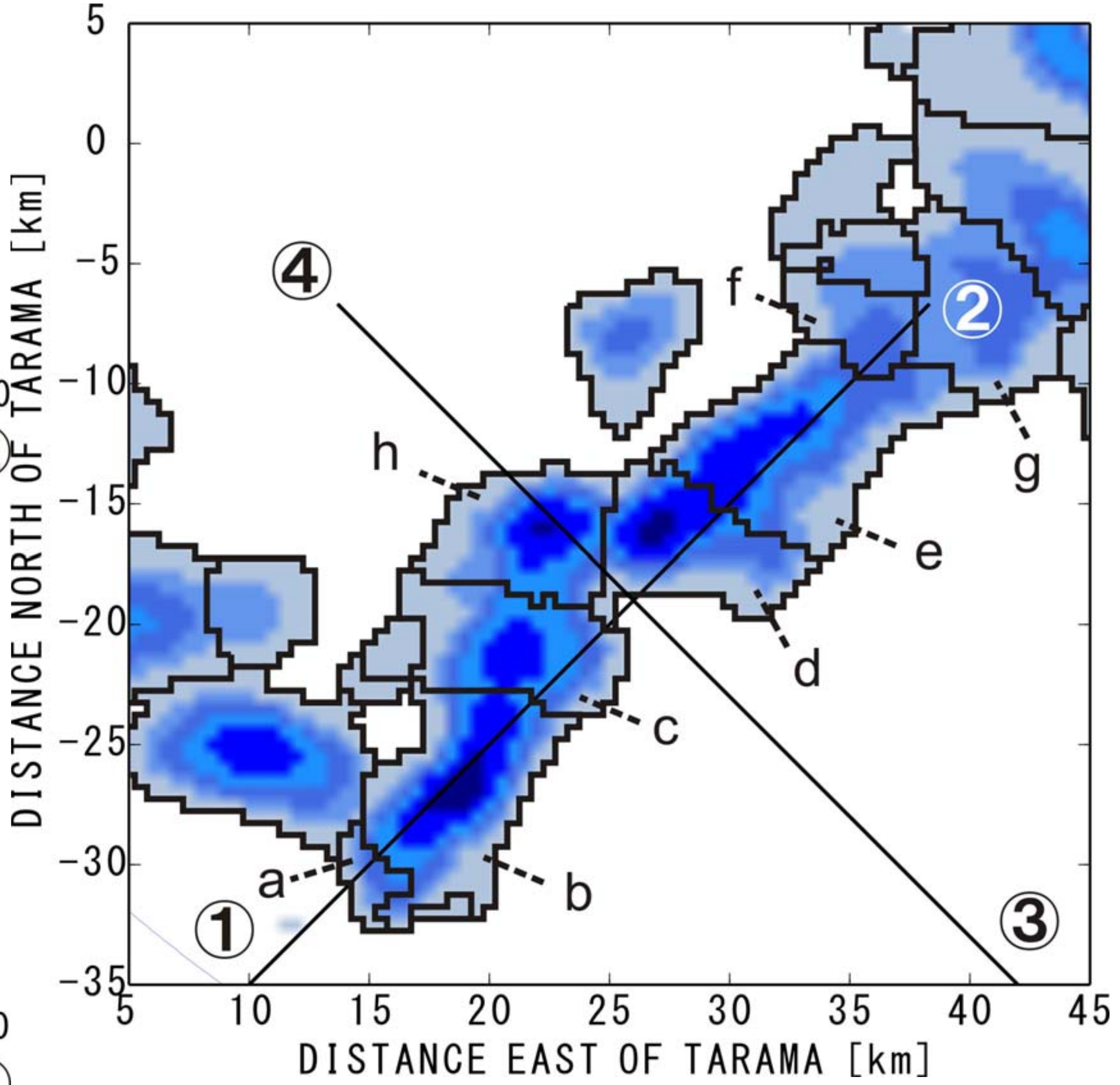

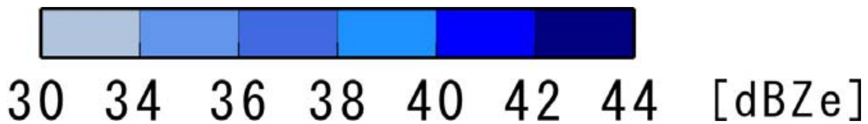

Precipitation cells are defined by spaces surrounded by a curved surface
(larger than 30 dBZe).

Detecting updraft and downdraft cells

- **Also, the second derivative for 3-dimensional wind velocity calculated from dual-Doppler analyses (Gao et al. 1999) can be calculated on each level.**
  *** Negative regions: the central part of updraft regions.**
  *** Positive regions: the central part of downdraft regions.**

→ The updraft and downdraft cells are defined by spaces surrounded by a curved surface (larger than 0.5 m/s of absolute wind speed)

Sample of Detecting Updraft and Downdraft Cells

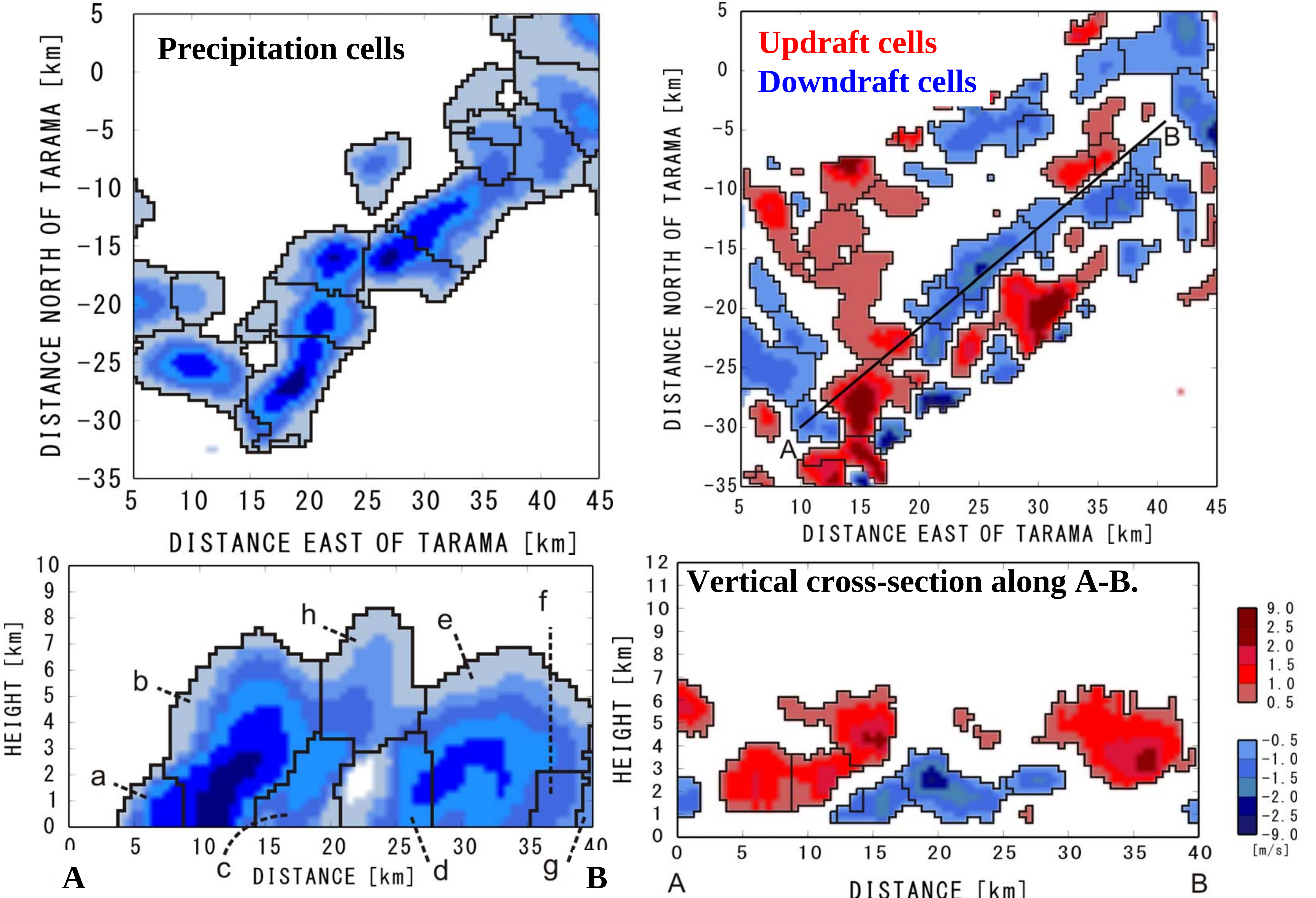

Definition of the Stages of Precipitation Cells

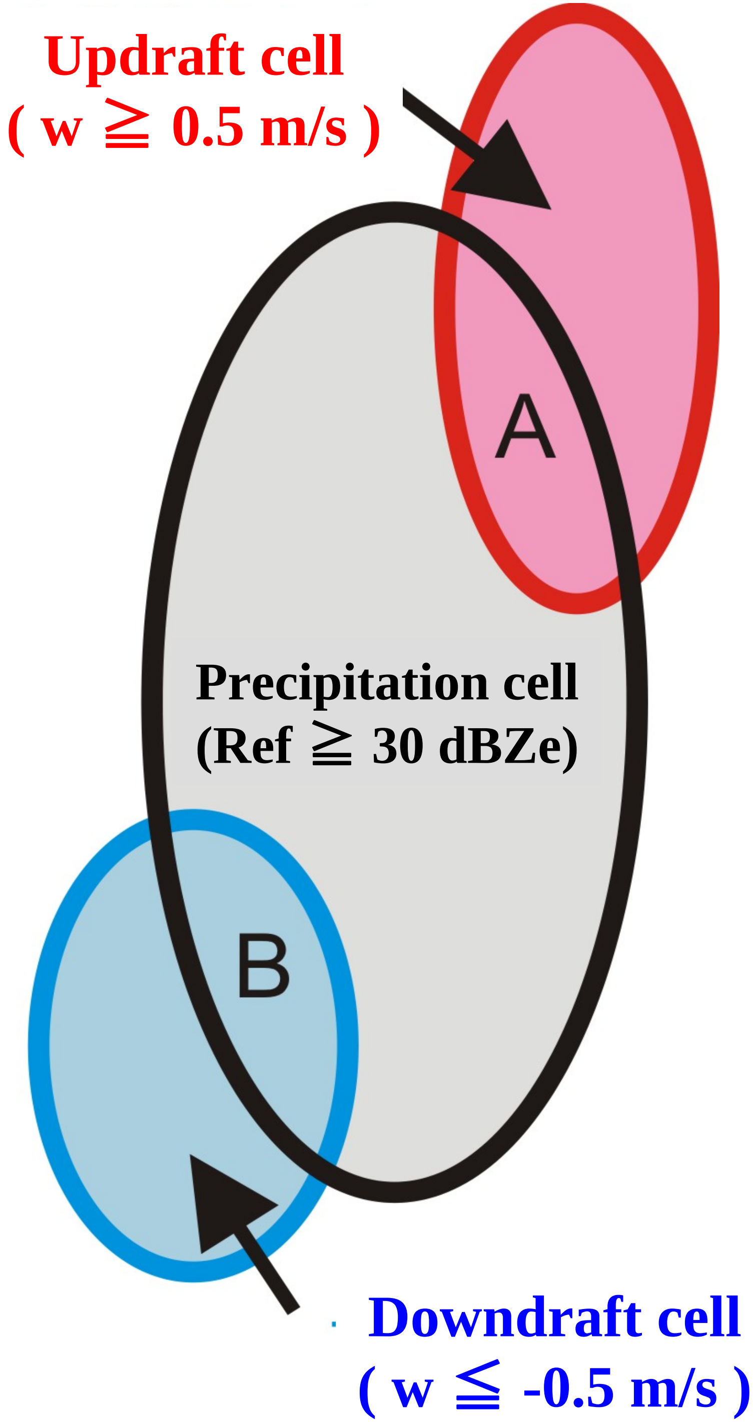

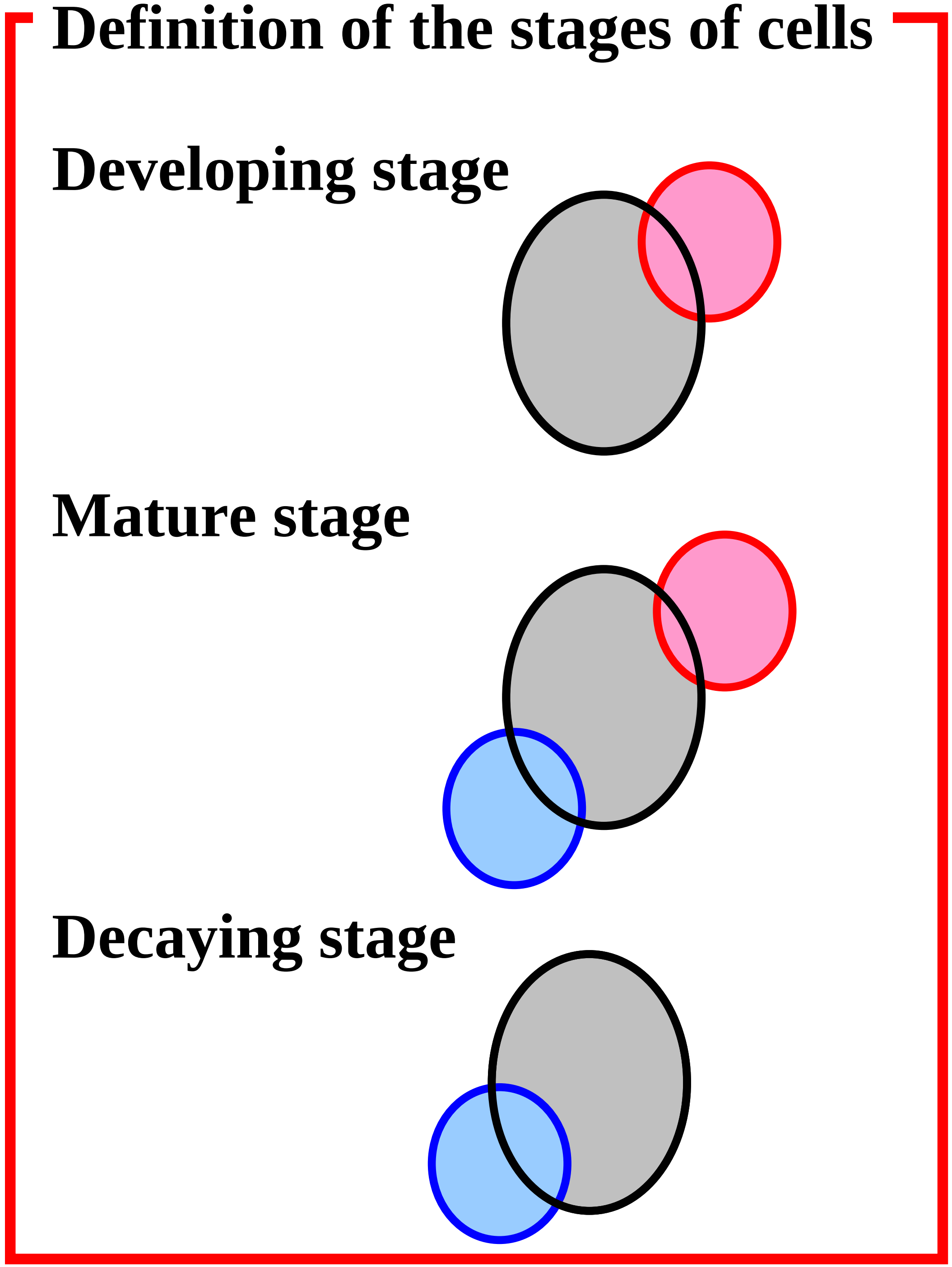

Time Series of Vertical Cross Section of a Chased Precipitation Cell

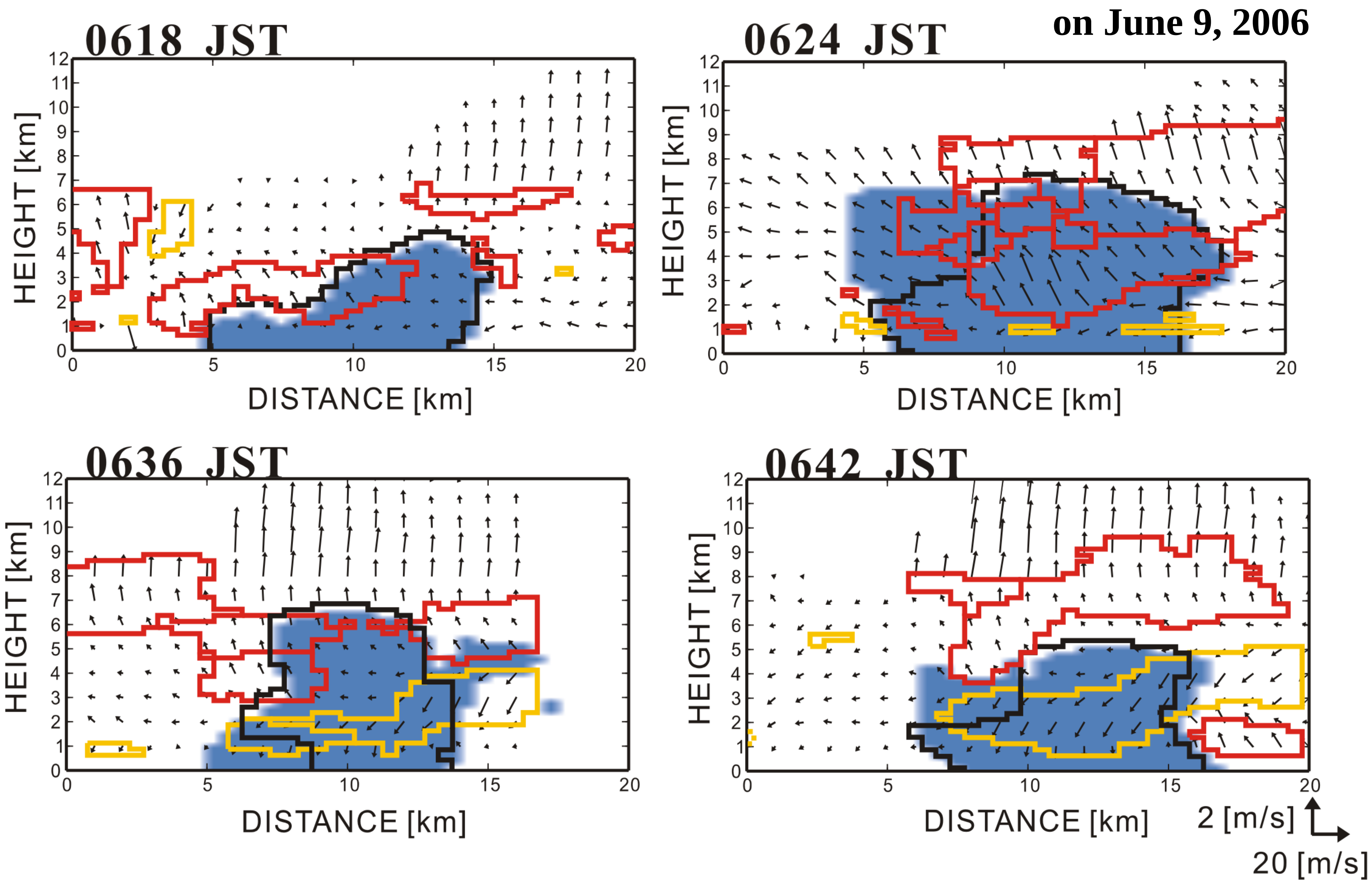

Trace of a Precipitation Cell to detect its Stages

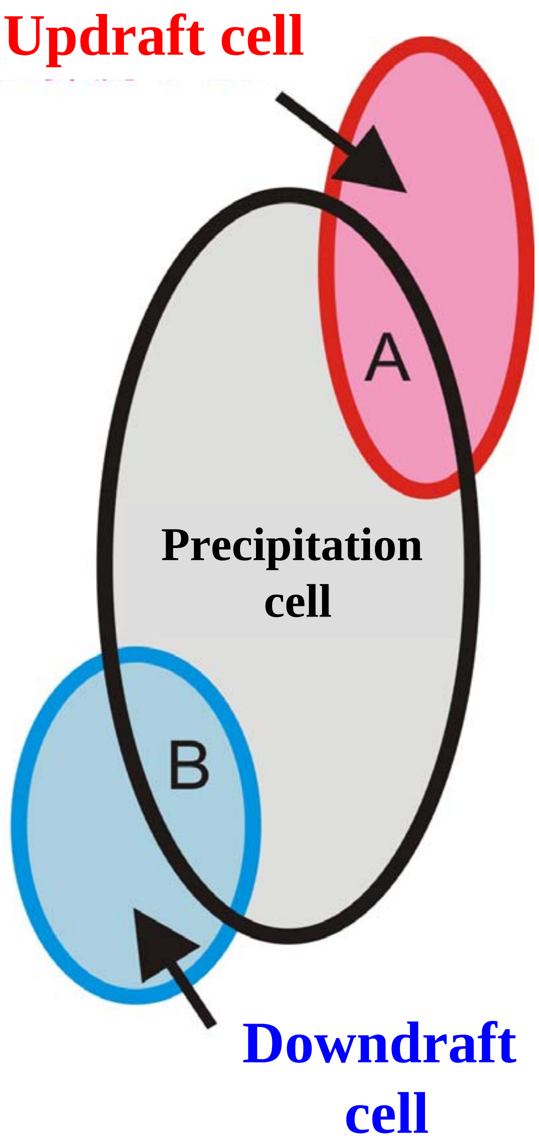

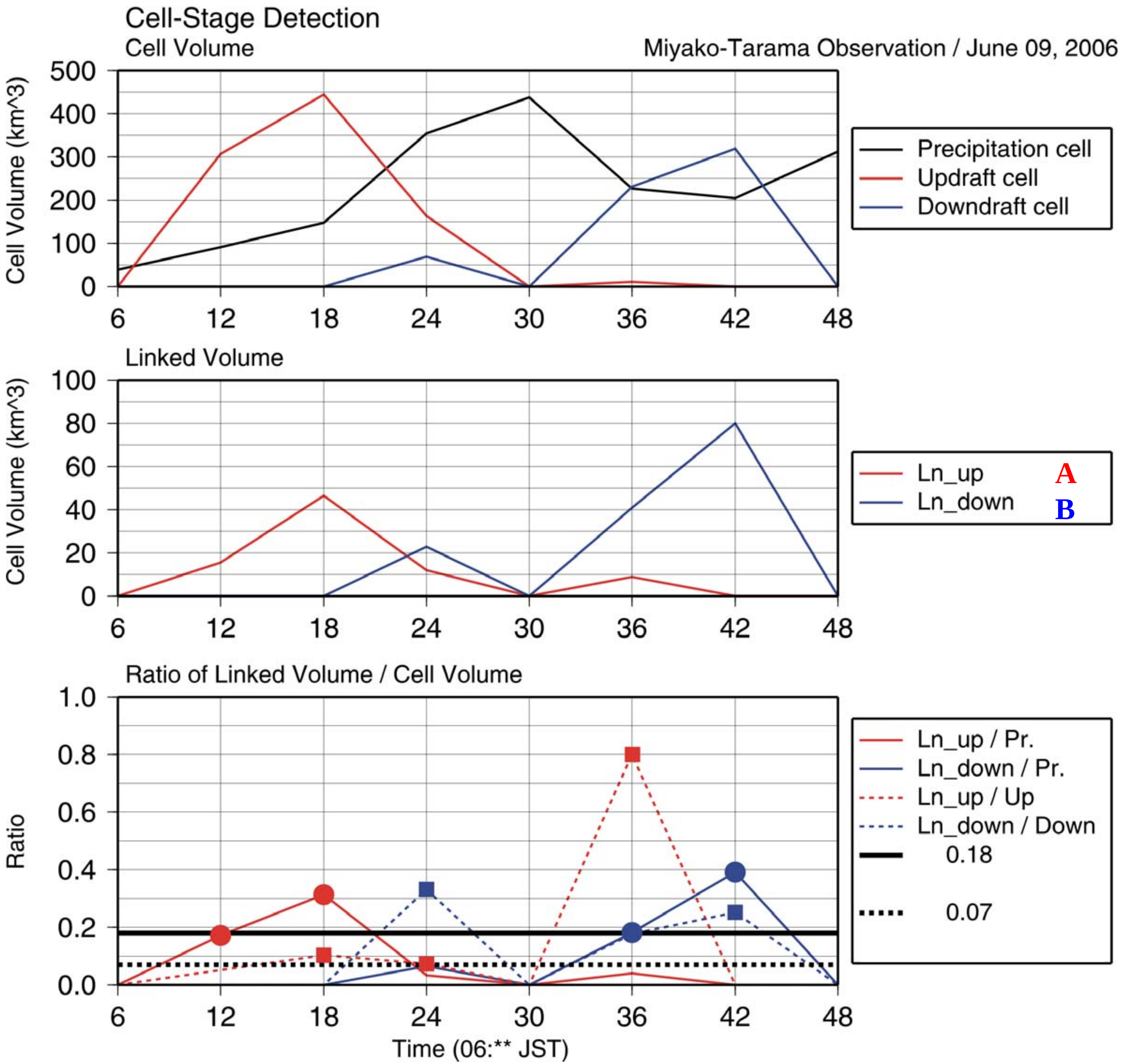

Definition of Connecting Precipitation and Updraft/Downdraft Cells

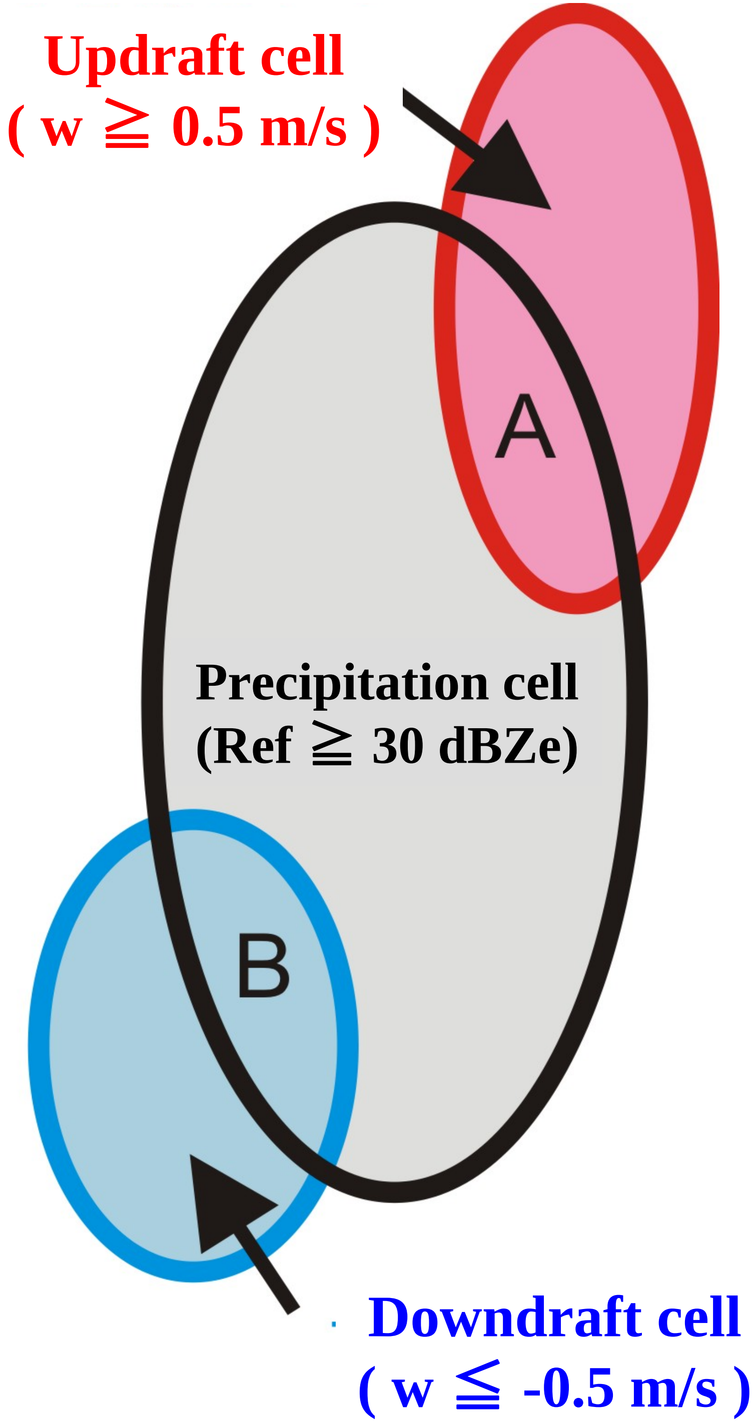

Connecting Precipitation and Updraft Cells

$$\frac{\text{Volume of A}}{\text{Volume of P.C.}} > 0.07$$

or

$$\frac{\text{Volume of A}}{\text{Volume of U.C.}} > 0.18$$

Connecting Precipitation and Downdraft Cells

$$\frac{\text{Volume of B}}{\text{Volume of P.C.}} > 0.07$$

or

$$\frac{\text{Volume of B}}{\text{Volume of D.C.}} > 0.18$$

Application of the Detecting Algorithm for Precipitation Cells

- **Number of cells of their stages**
  - **The observation data are 55 volume scanning data from 0036 to 0918 LST on June 9, 2006.**

Stages	Numbers of cells
Developing stage	183
Mature stage	154
Decaying stage	124

Vertical Profiles of Averaged Area of Precipitation Cells

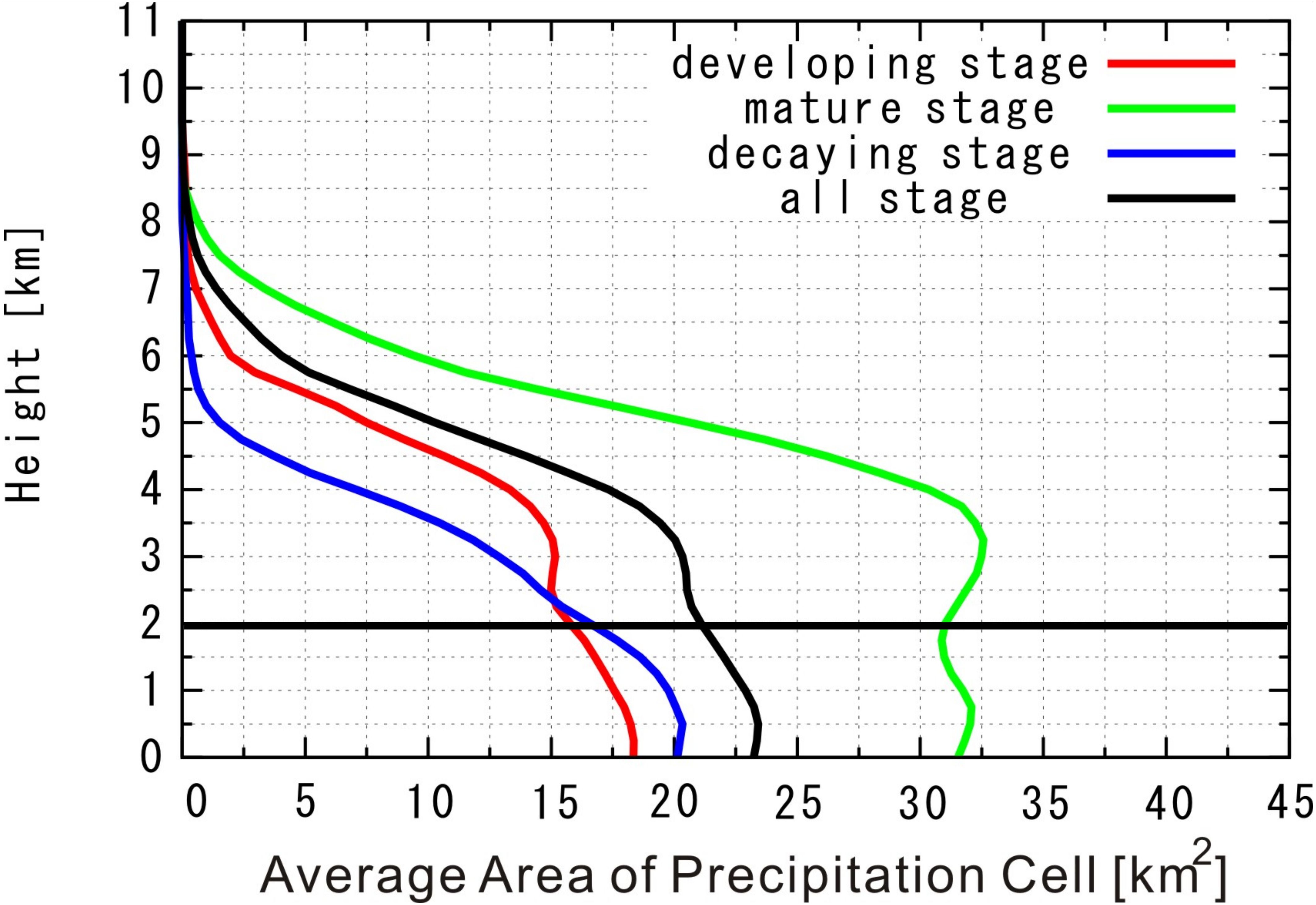

Integrated Probability Density of Area of Precipitation Cells

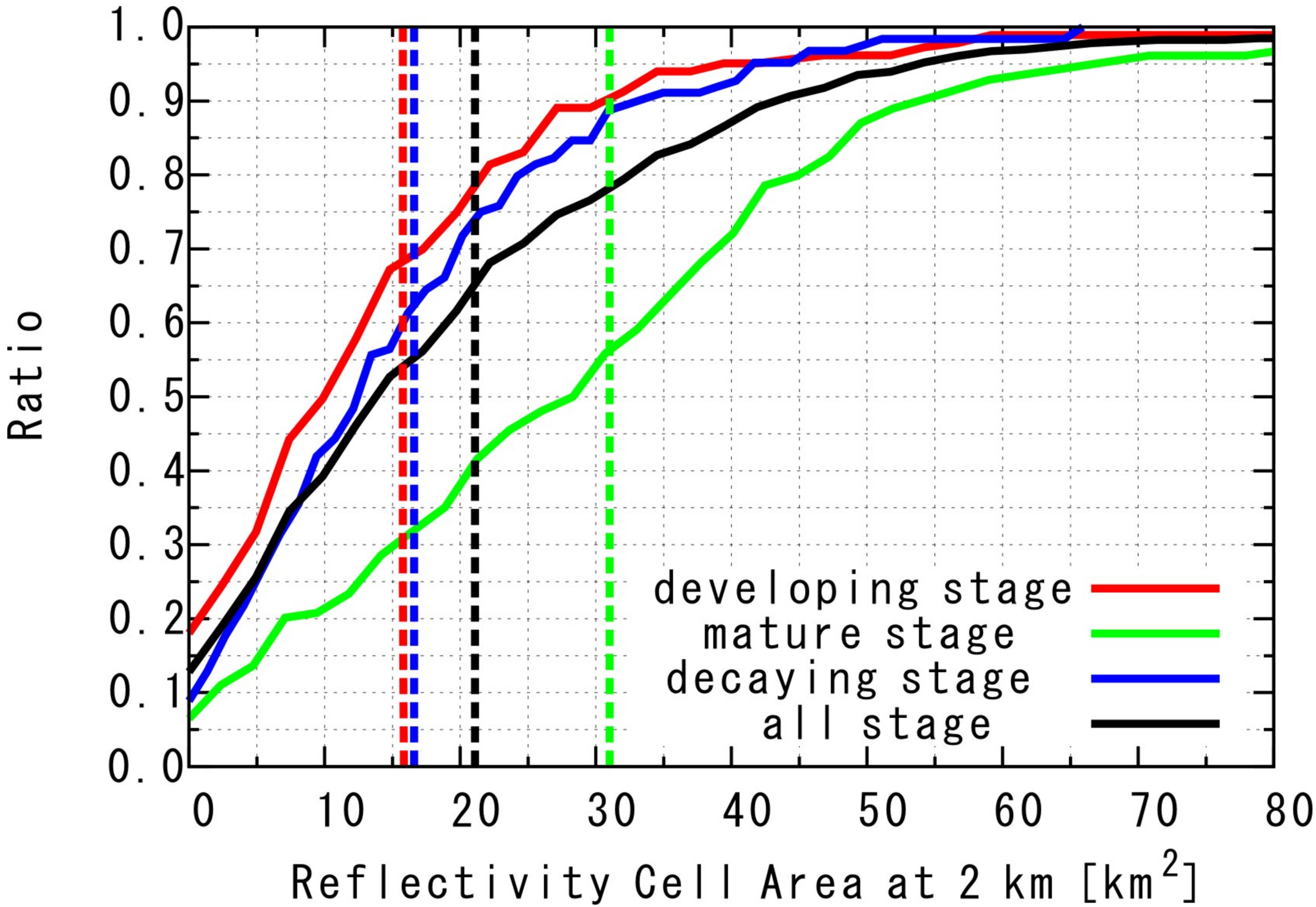

Integrated Probability Density of Echo-top Height of Cells

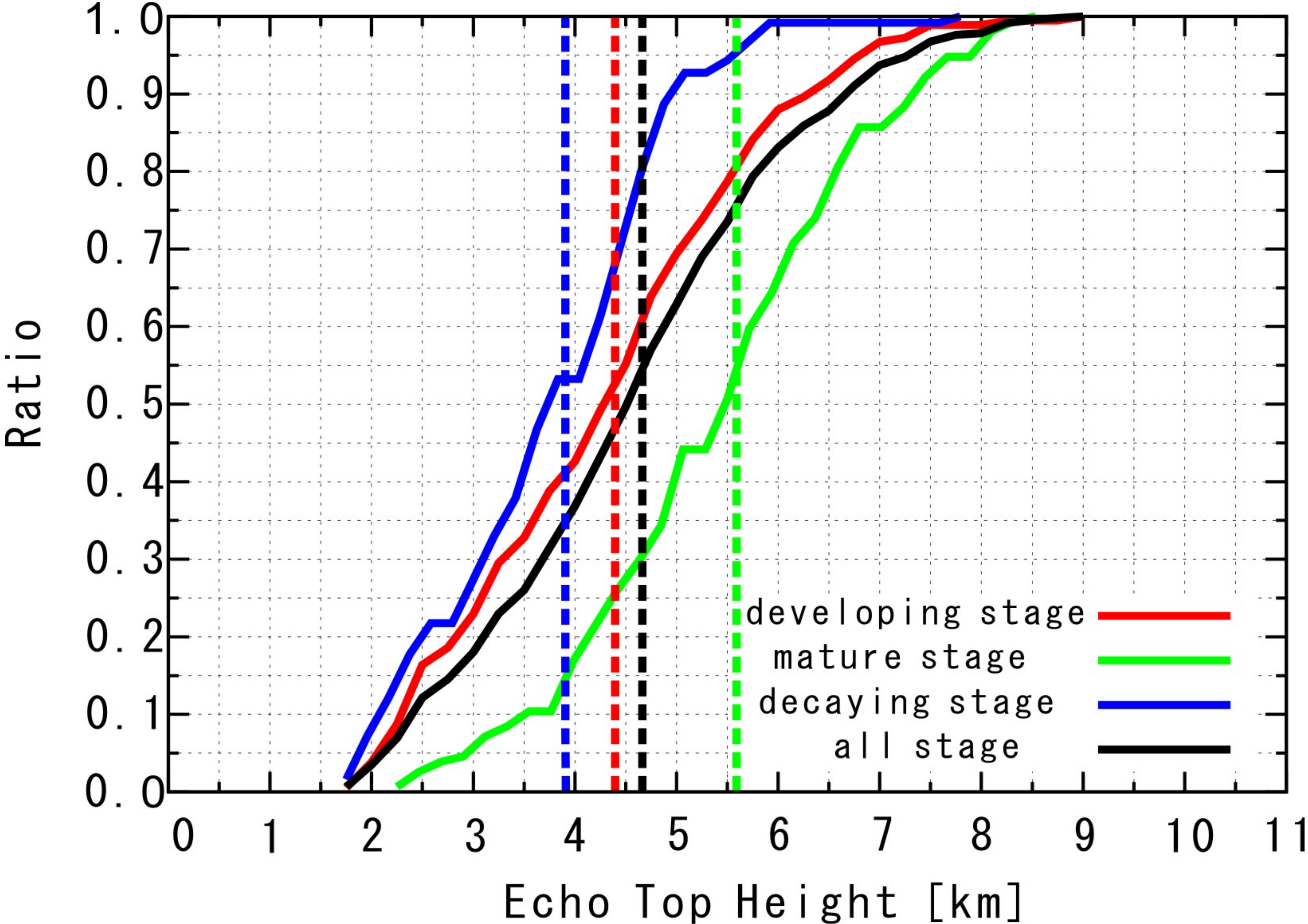

Summary

- **We develop a three-dimensional detection algorithm for "precipitation cells" using reflectivity data.**
- **The algorithm can also detect "updraft cells" and "downdraft cells" to apply three-dimensional wind field data calculated from dual-Doppler analyses.**

→ Matching up the precipitation cells with updraft and downdraft cells marks the developing, mature, and decaying stages in their life-cycle.

- **We can present statistical features of each stage of precipitation cells observed around the Baiu front in 2006.**
  *** Averaged area**
  *** Echo-top height**

- **The information of stages of precipitation cells should be useful for understanding the structure of precipitation systems.**
- **We are also developing the tracing algorithm for cells.**

Backup

Numbers of Detecting Precipitation Cells

Observation Area	Number of Cells
Shouxian (mainland China: continental, 1998)	23,915
Zhouzhuang (coastal area, 2001)	7,573
Tarama (Okinawa, oceanic, 2006)	1,508

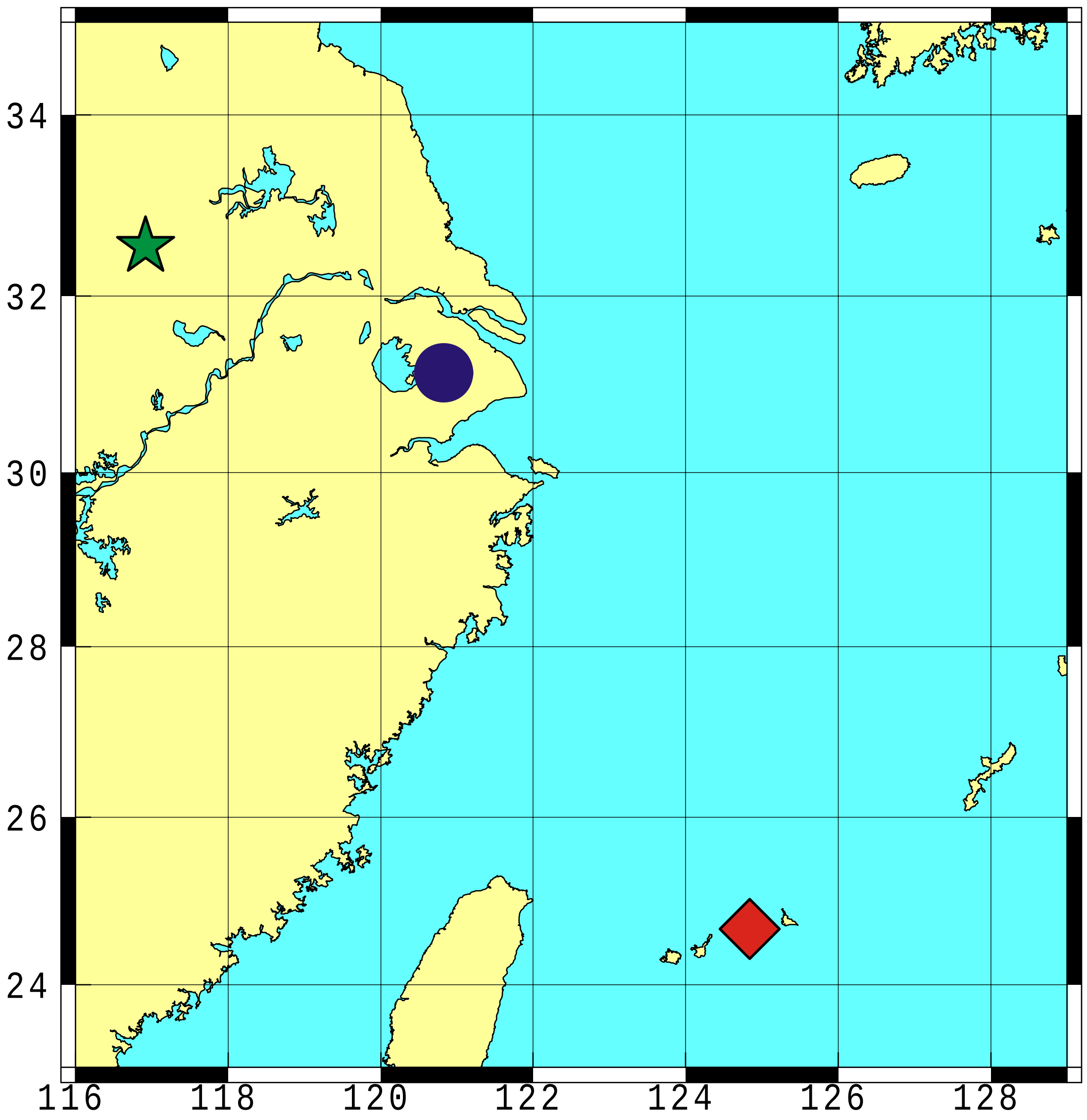

Integrated Probability Density of Echo-top Height in Each Area

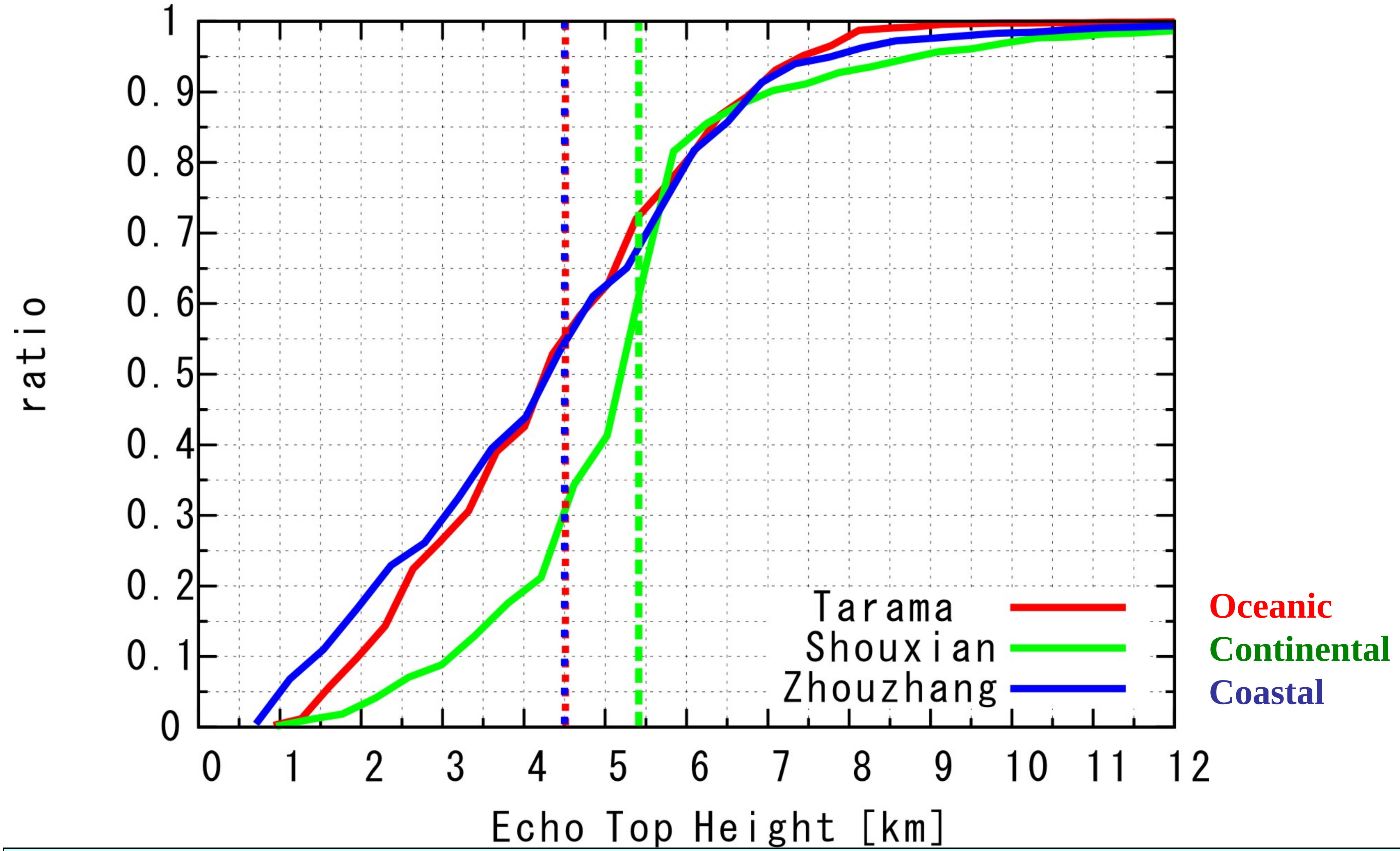

- **Echo-top height of precipitation cells is quite low: Height less than 6 km occupies 80%.**

Vertical Profiles of Averaged Cell Area in Each Area

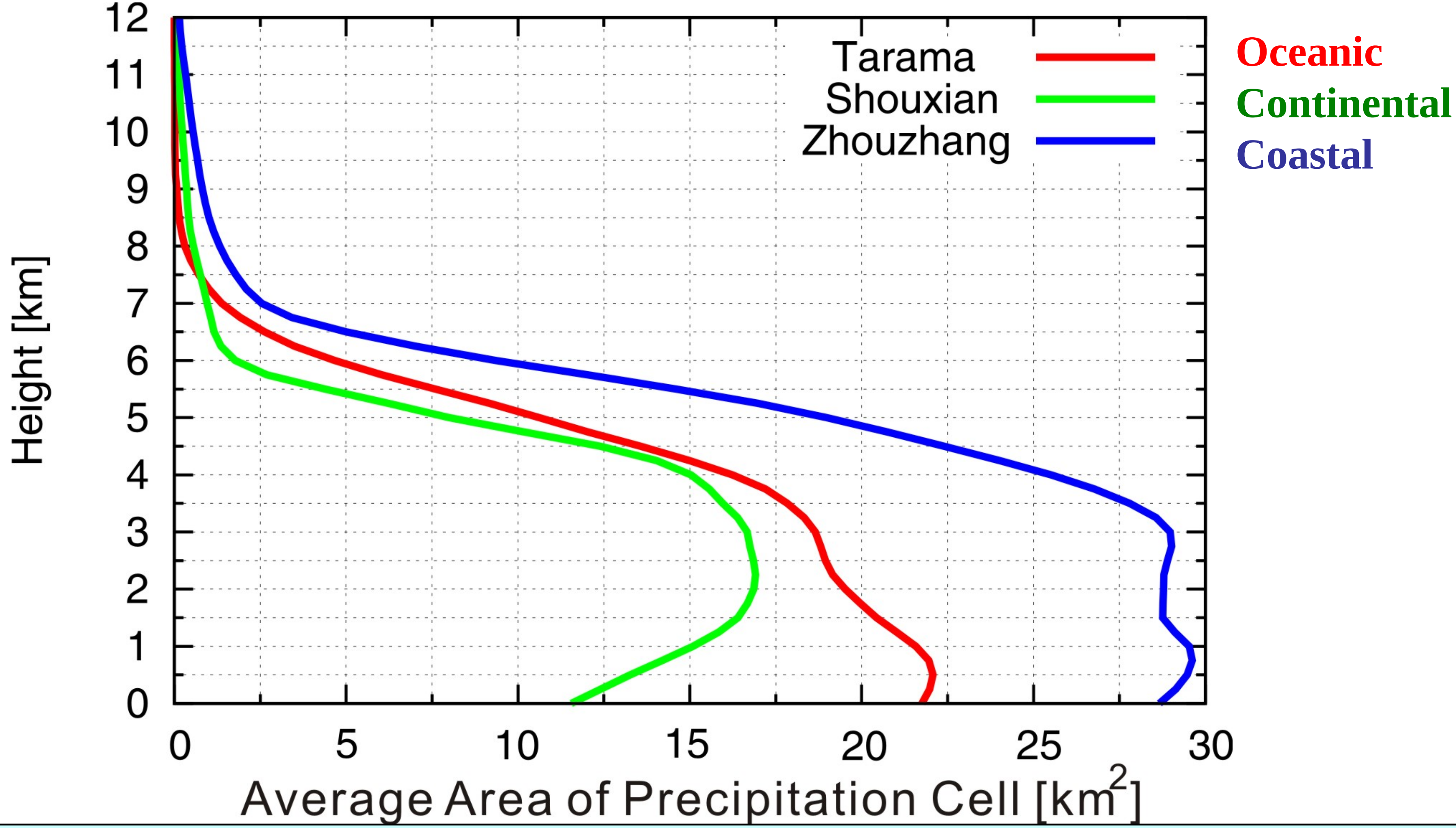

- **Averaged cell area is less than 30 km2 (Zhouzhuang), 20km2 (Shouxian).**
- **Averaged cell area at Shouxian increase with height.**
- **That at Tarama decrease with height.**

→ Reflectivity profile is also same.

発達段階を識別するための降水セルの追跡

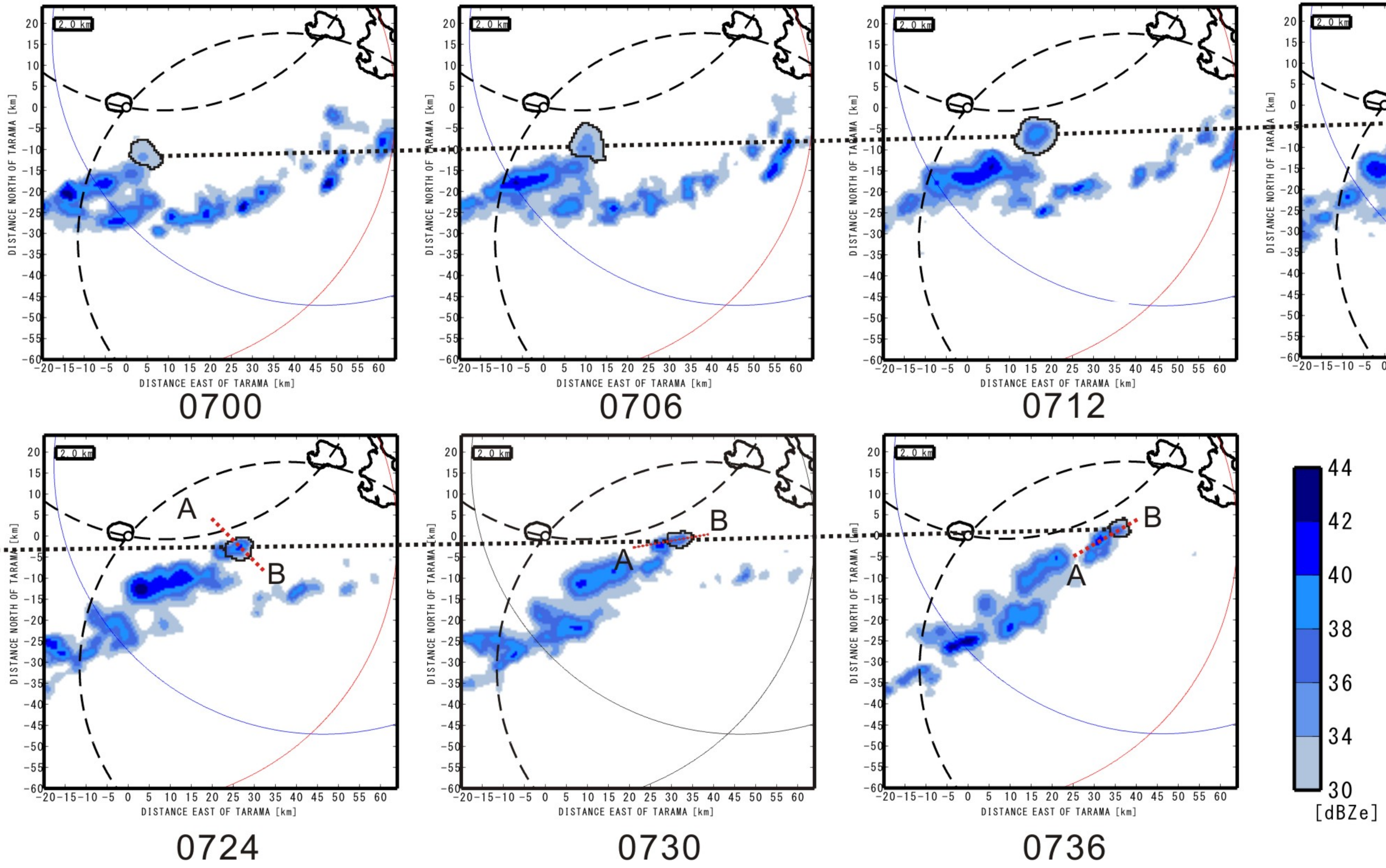

2006年6月9日07時00分から07時36分に観測された降水セルを高度2 kmの水平断面で追跡。

発達段階を識別するための降水セルの追跡

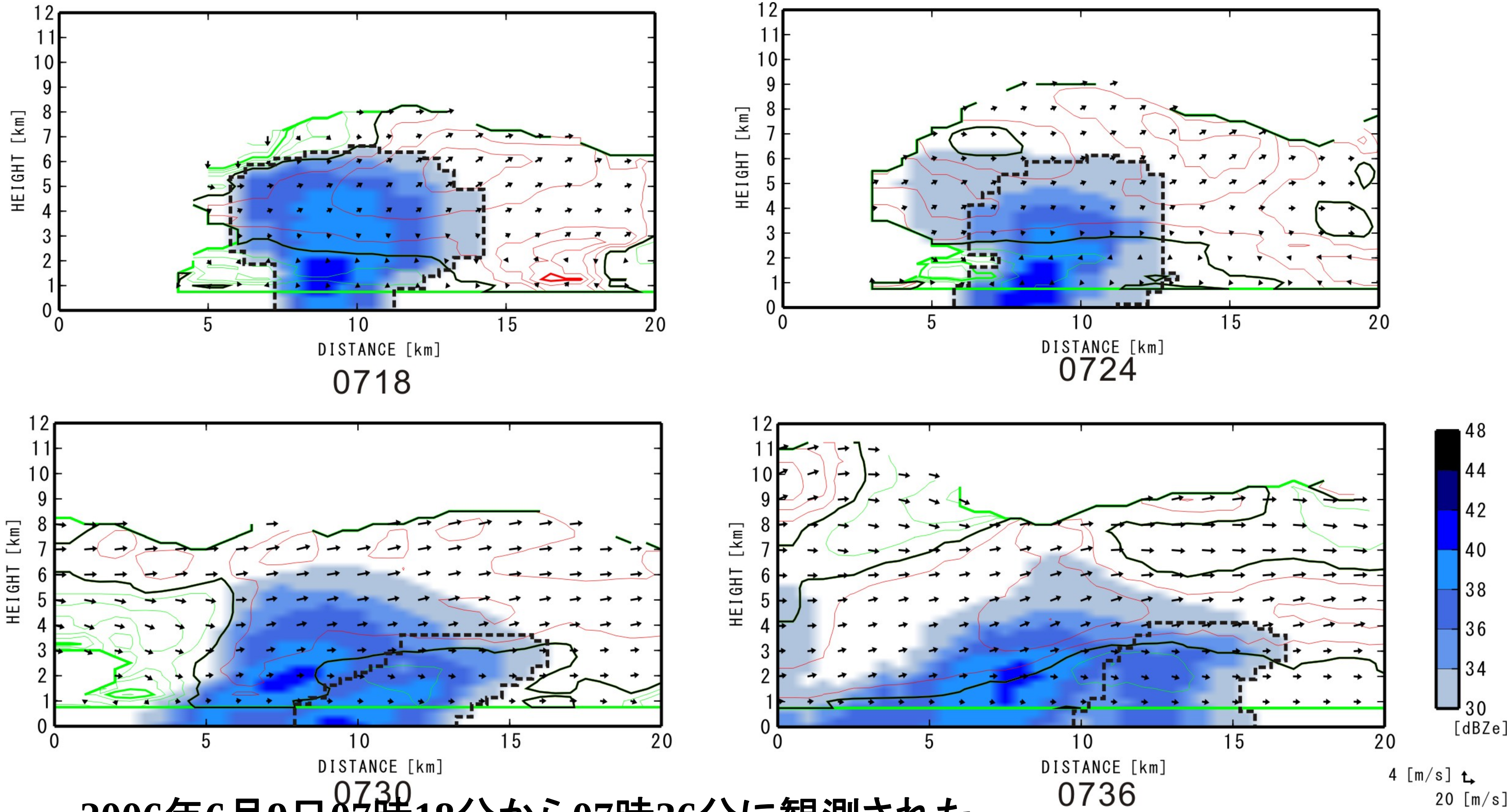

2006年6月9日07時18分から07時36分に観測された降水セルを鉛直断面で追跡。

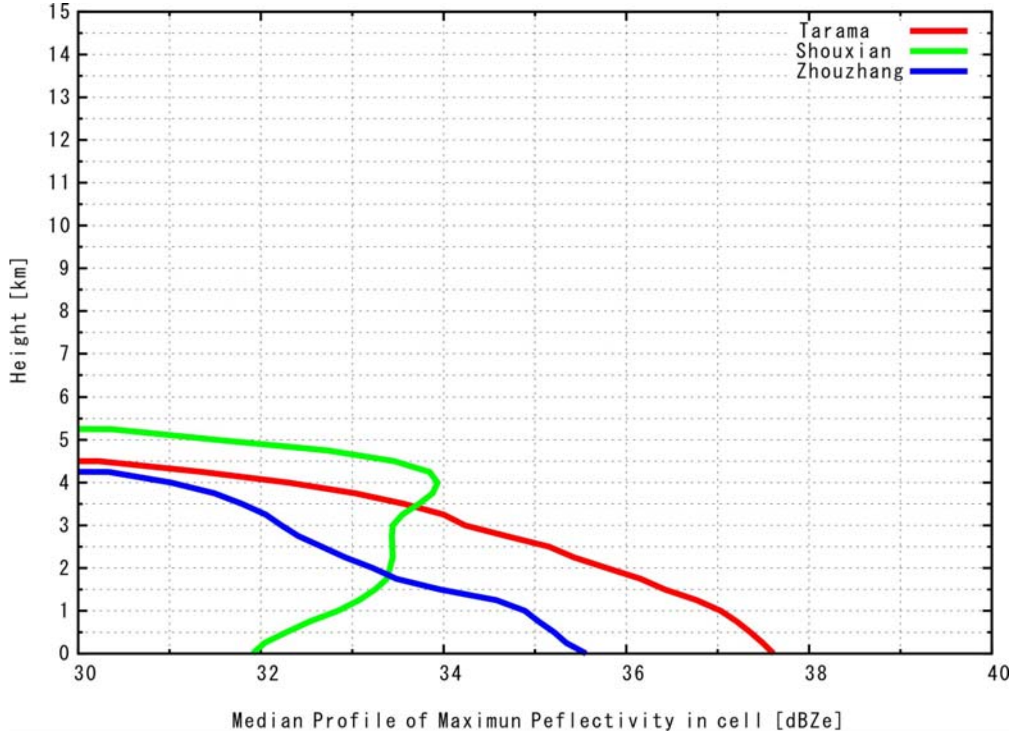

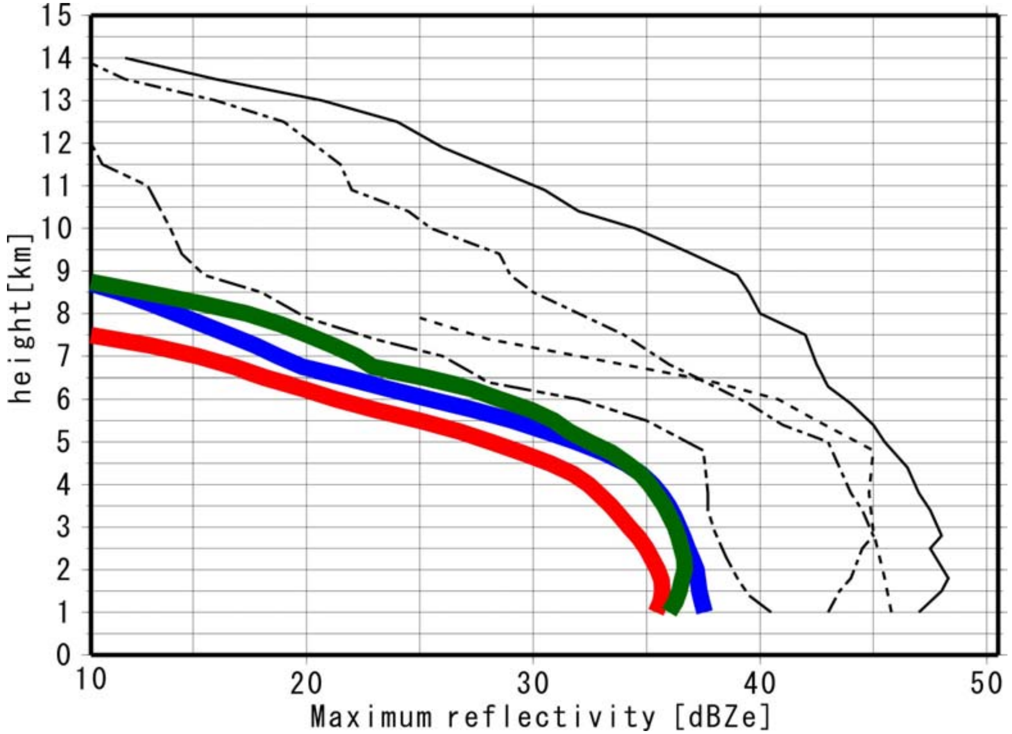

赤　　　　:多良間島、沖縄(海洋性)
緑　　　　:寿県(大陸性)
青　　　　:周庄(沿岸部)
実線　　　:オクラホマ(大陸性)
破線　　　:台湾(海洋性)
一点鎖線:ダーウィン(大陸性)
二点鎖線:ダーウィン(海洋性)

下図の赤、緑、青線:真木,2007
　　黒線　　　　:Zipser and Luts 1994
より

発達段階を識別するための降水セルの追跡（セル体積の時系列）

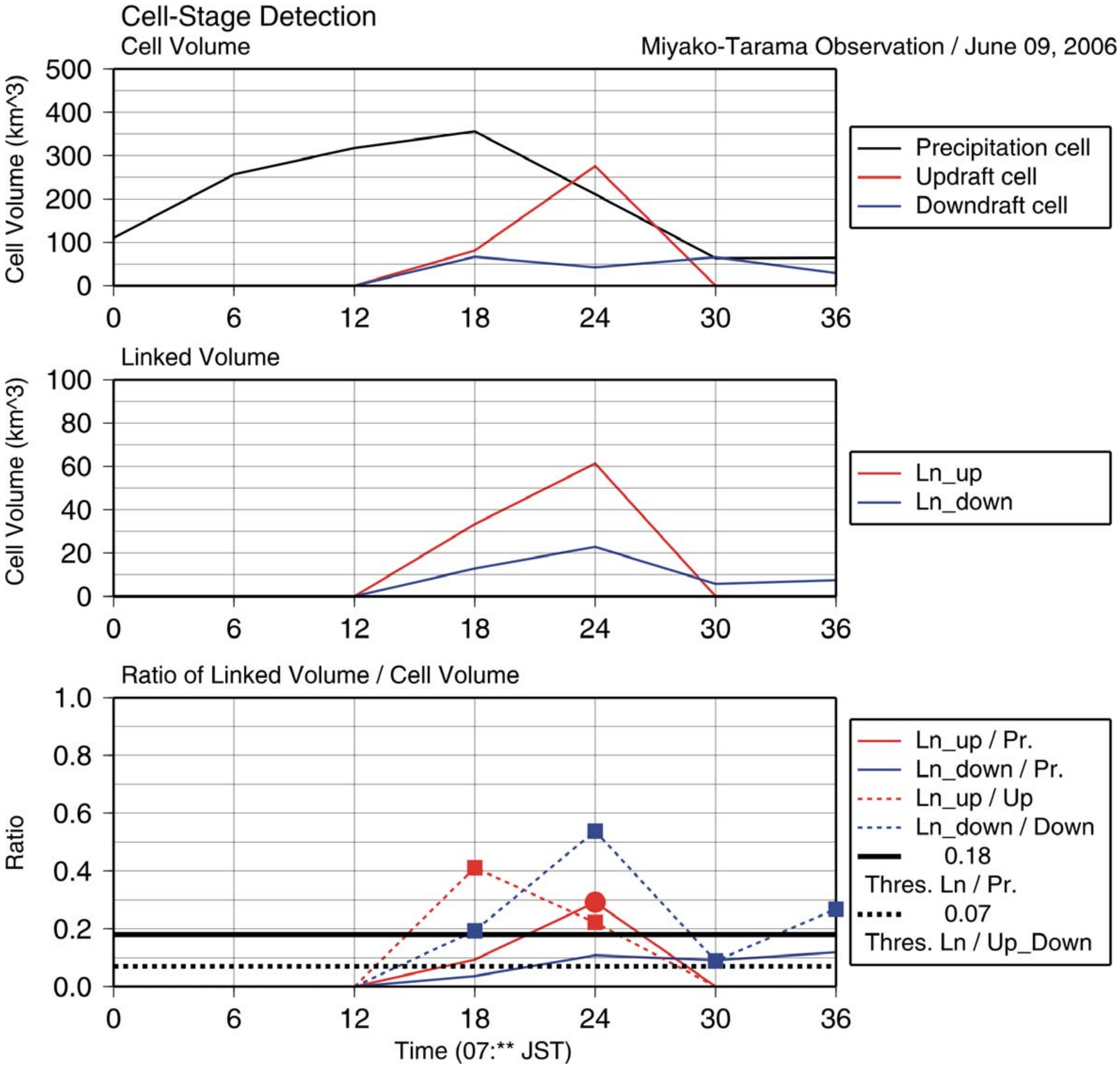

Integrated Probability Density of Volume of Precipitation Cells

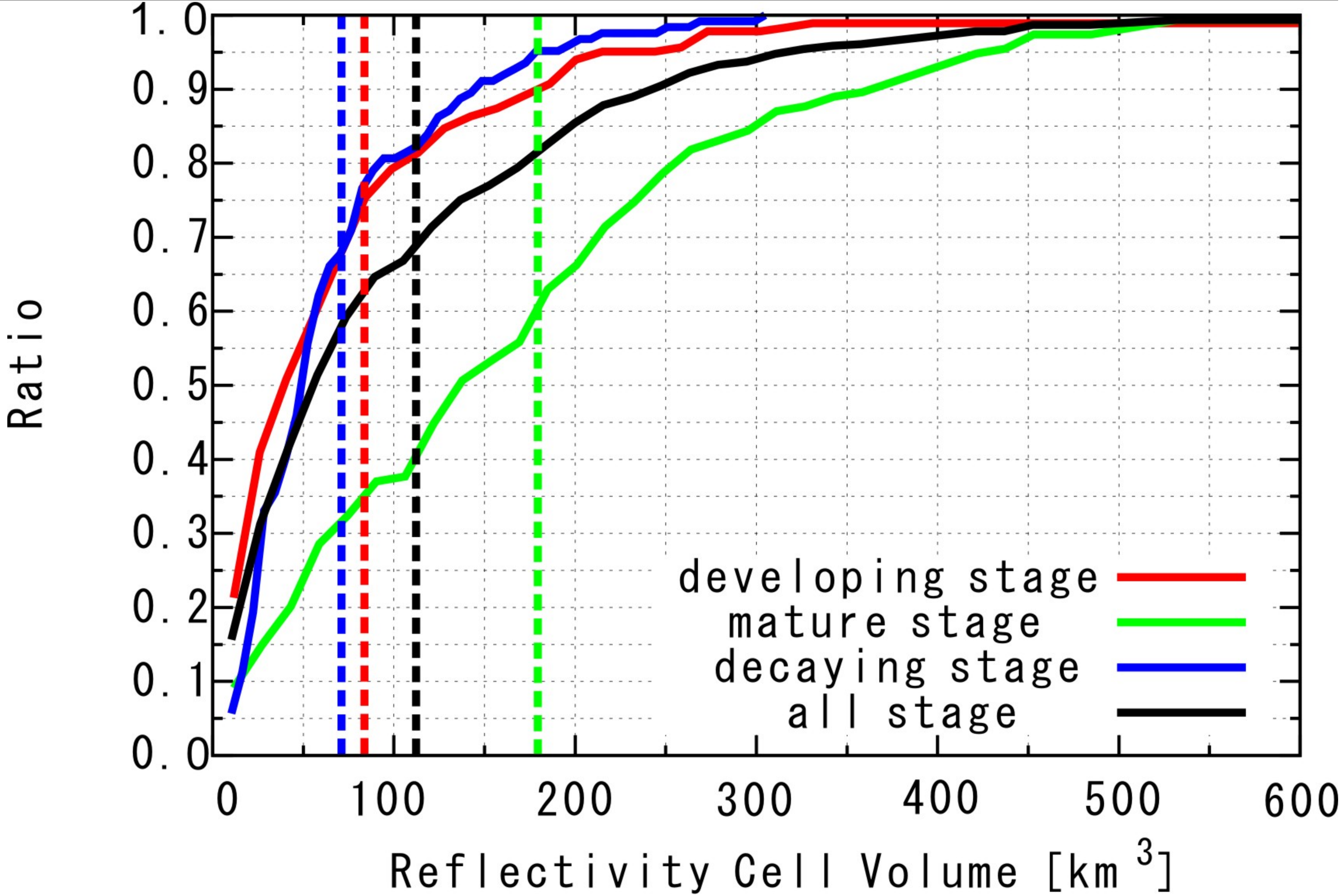

Backup（深町オリジナル）

2. アルゴリズムの概要

使用するデータ

PPIデータ（極座標系データ）を内挿して作成した、反射強度の3次元格子（CAPPI）データ。

PPIデータ

距離分解能: 250 [m]

ビーム幅　:1.2[°]　距離補正、減衰補正（Battman, 1973）済

Battmanの方法　$Ka = 1.12\times10^{-4} Z^{0.62}$

Ka:減衰率[dB/km] Z:レーダ反射因子[mm^6/m^3]

２. アルゴリズムの概要

PPIデータの各格子点を中心とする楕円影響球を設定し、
楕円球の内部にあるデータに中心からの距離を用いた重み関数をかけ、
荷重平均を行う。Cressman (1959)

重み関数設定
$$W = \frac{1.0}{1.0 + \alpha(\frac{d^2}{K^2})}$$

$$K = \sqrt{K_h^2 + K_v^2}$$
α ＝9.0

$$K_h = 1.5 \qquad K_v = 1.0 \qquad (el \leq 4.9)$$

$$K_h = \frac{1}{30}(r - 30) + 2.5 \qquad K_v = \frac{1}{60}(r - 30) + 1.5 \qquad (4.9 < el \leq 8.8)$$

$$K_h = \frac{1}{30}(r - 30) + 3.5 \qquad K_v = \frac{1}{60}(r - 30) + 1.5 \qquad (8.8 < el)$$

d は極座標系のデータ点と3次元直交座標系のデータ点との距離
r はレーダーからの距離

闘値 30[dBZe]の設定方法について

dBZe	Z	mm/h (Marshall, 1955) Z = 200 R ^1.6	mm/h (Sekhon,1971) Z= 300 R ^1.35
31	1259	3.16	2.89
30	1000	2.73	2.41
29	794	2.36	2.05
25	316	1.33	1.04
23	200	1.00	0.74
20	100	0.65	0.45

2. アルゴリズムの概要

BBF(: Bright Band Fraction)法
(Rosenfeld and Buffalo, 1964　Chen and Uyeda, 2003)

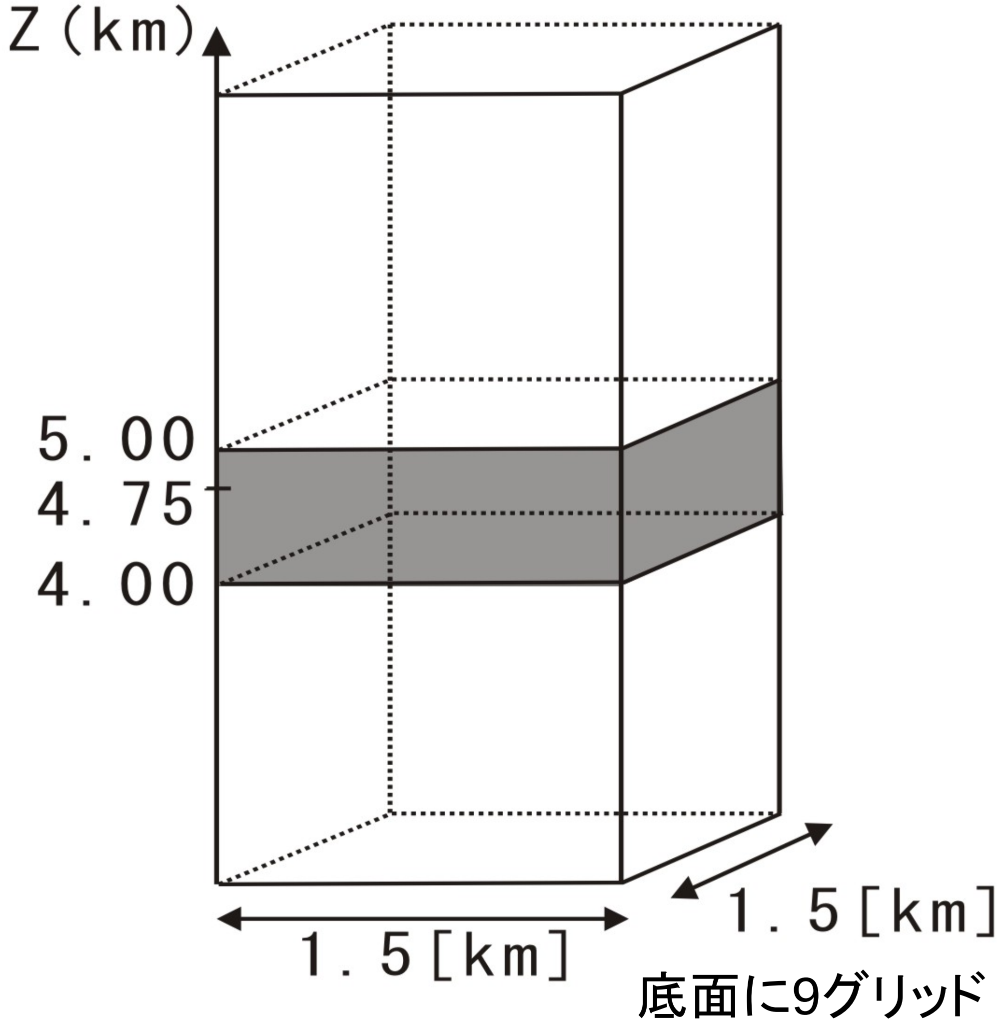

高度4[km]の水平断面図

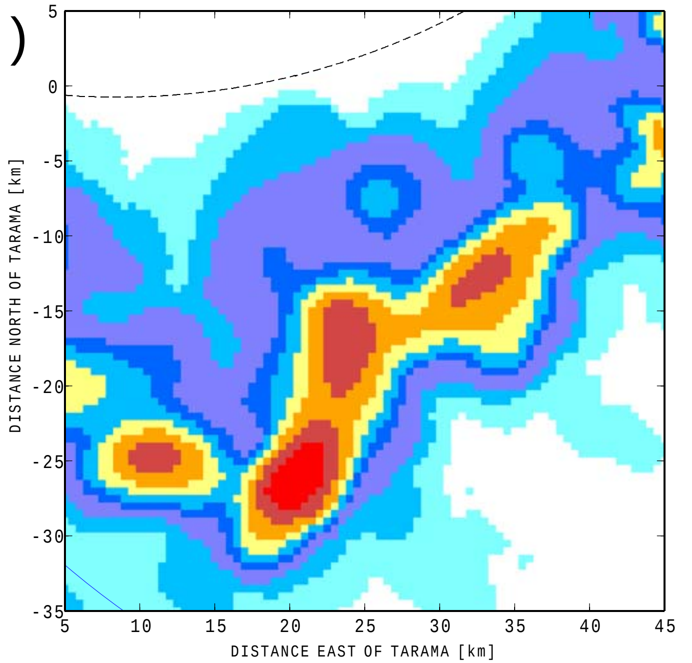

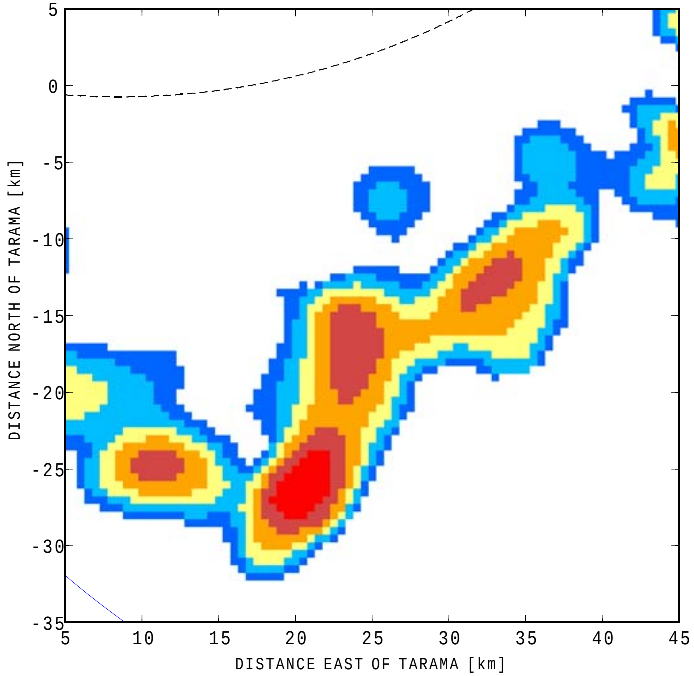

BBF ≧ 0.6 のカラムを層状性降水域として除去する

2. アルゴリズムの概要

2階微分への入力データについて

$$\Delta F(x) = 2\left[\frac{F(x+1) - F(x-1)}{2} - F(x)\right]$$

注) 反射強度 = 10 × log(反射因子)

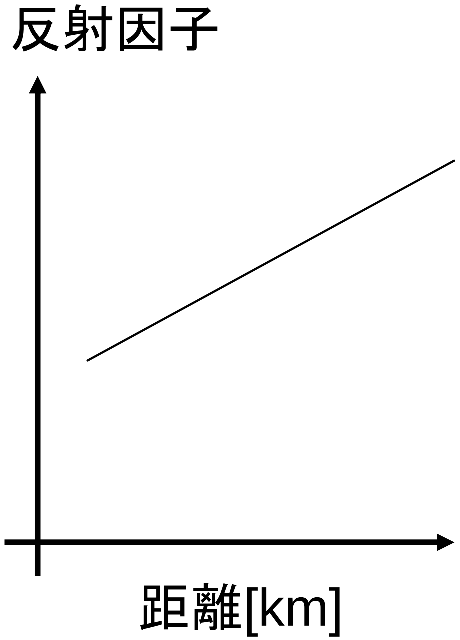

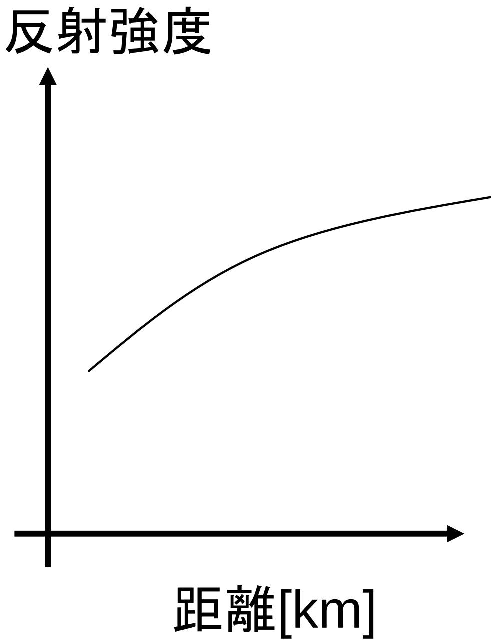

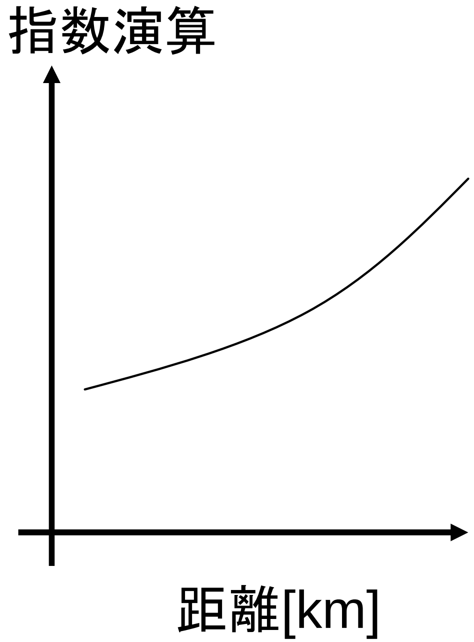

2階微分が0の
反射因子の分布

反射強度の
2階微分は負

指数演算の場合
2階微分は正

セルとセルが分離するために、
地域、レーダ、CAPPIデータの空間分解能に
対して、最適な演算を選択する必要がある。

2007年の沖縄の場合：

Input (: Ref *) = $10^{Ref / 5.0}$

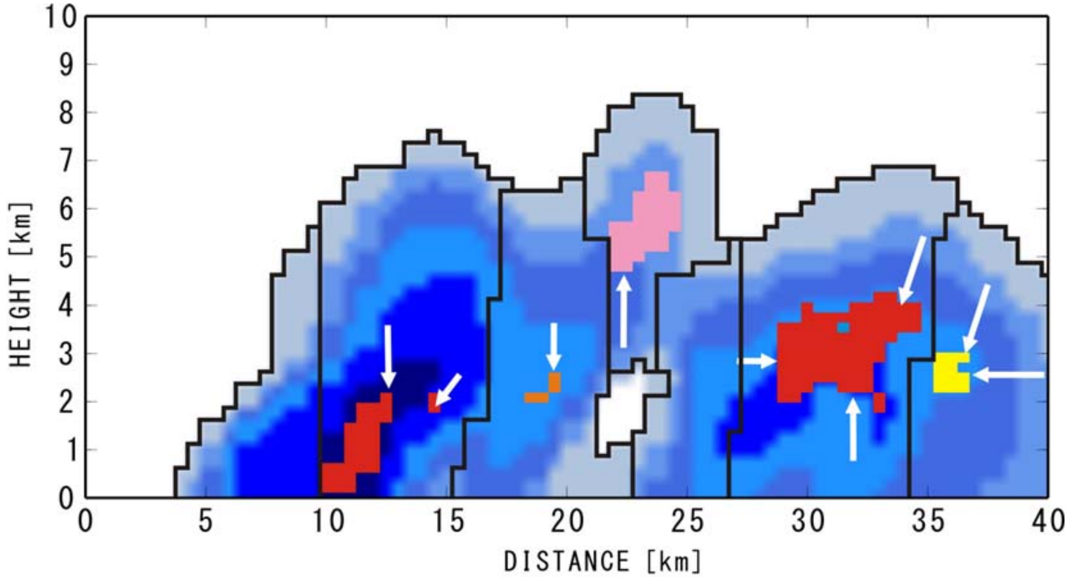

	A	B	C	D	E
1	34	33	32	32	33
2	34	34	33	32	33
3	35	34	33	33	33
4	34	33	32	33	34
5	35	33	33	34	34

1	34	33	32	32	33
2	34	34	33	32	33
3	35	34	33	33	33
4	34	33	32	33	34
5	35	33	33	34	34

アルゴリズムの精度検証

降水セルの誤検出の原因の大半は飛び地であった。
どういう領域かというと・・・

30 dBZe以上だが、
２階微分が計算できない
程度の大きさの領域。
降水セルと判定されない。

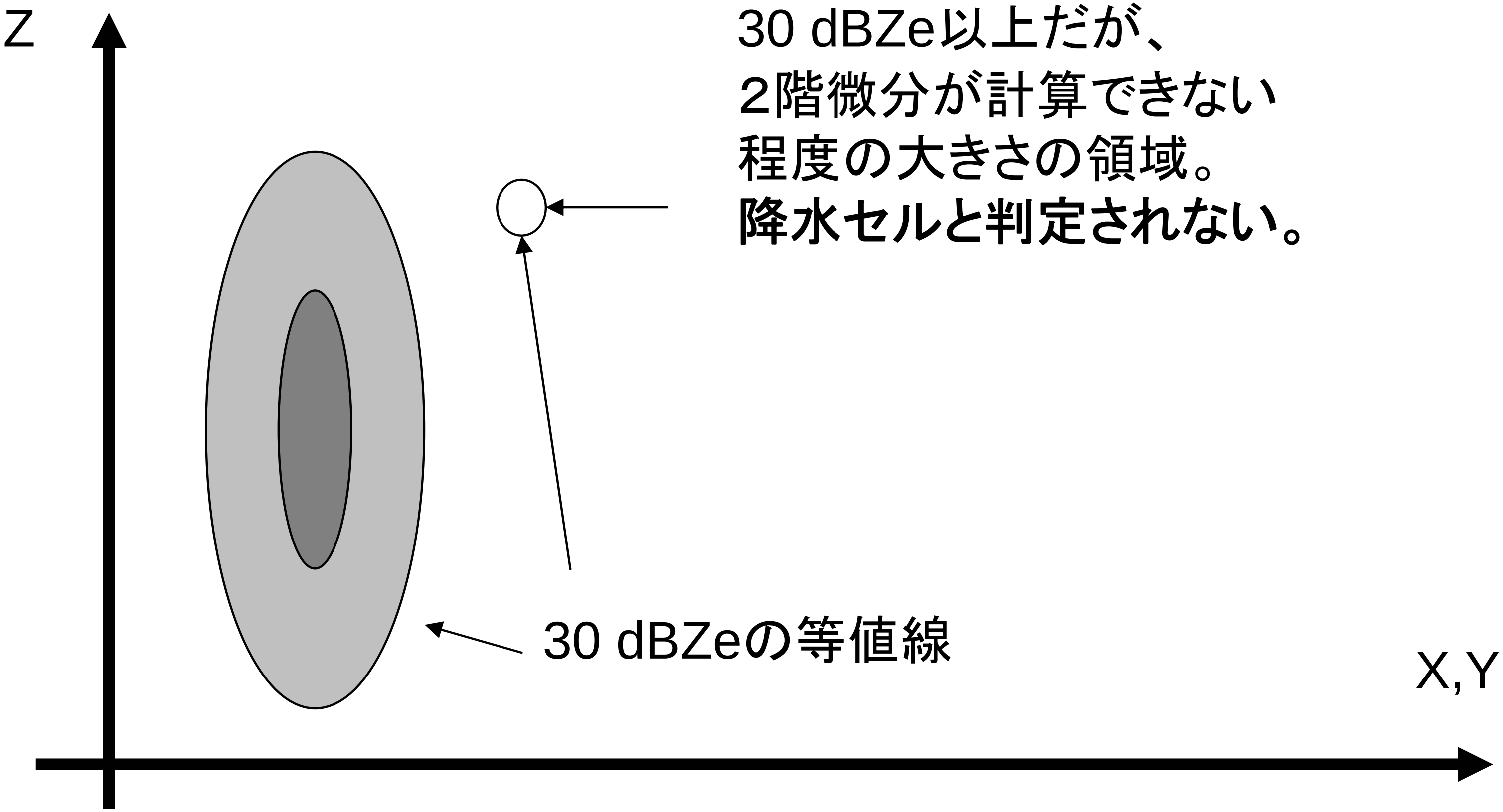

アルゴリズムの課題

飛び地を持たないようにするために、改良する必要がある。
２階微分を計算できない領域があるのが問題

現状
1. 閾値以下の反射強度のデータを消す。
2. ２階微分を計算する。
3. 降水セルのラベリングを行う。
4. 中心部以外の領域を配分する。
5. 小さすぎる降水セルを消す。

改善方法
1. ２階微分を計算する。
2. 閾値以下の反射強度のデータを消す。
3. 降水セルの中心部のラベリングを行う。
4. 中心部以外の領域を配分する。
5. 小さすぎる降水セルを消す。

どの降水セルの領域にしていいか分からない領域の
扱い方の検討

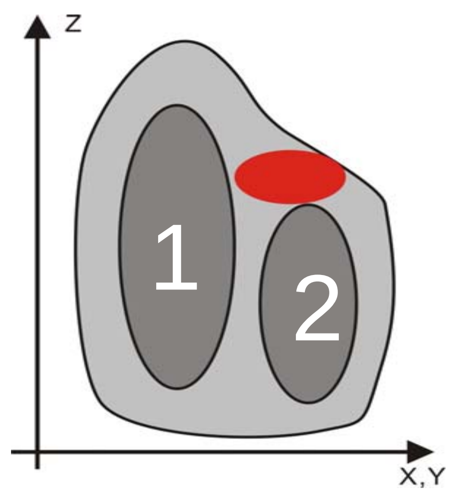

発達段階の判別時の閾値

時刻(地方時)	気流構造から判別した結果	体積、面積、反射強度からの判別	アルゴリズムの判別結果
0700	不明	発達期	不明
0706	不明	発達期	不明
0712	不明	発達期か成熟期	不明
0718	成熟期	成熟期	成熟期
072			熟期
073			退期
073			退期

一般的な閾値を決めるためには、
もっと事例数を増やして、
３種類のセルのリンクの条件や
閾値を検討する必要がある。

注）デュアル領域から１格子点でもはみ出している降水セルの発達段階は不明とした。

ステージ間の特徴の比較

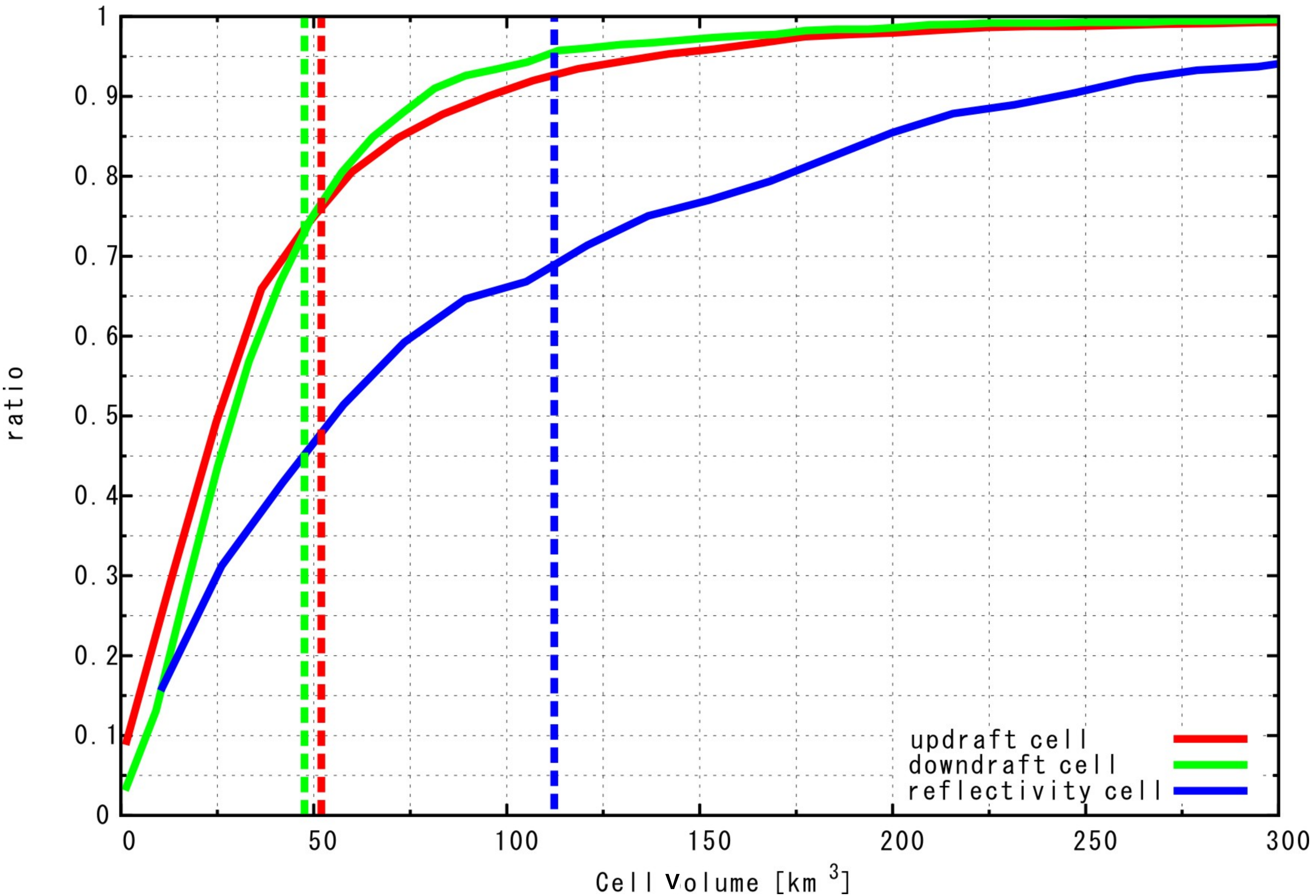

今後の課題

● 今後の課題

- 発達段階を規定するための降水セルと上昇流セル・下降流セルが重なり合う部分の体積の割合に対する適正な値は、今後、ケースを増やして検討を行っていく必要がある。

- 降水セルの追跡アルゴリズム（清水他 2005 秋季大会 P380など）と組み合わせて使用することにより、降水システム内部における降水セルの発生から消滅までの統計的な特徴を得ることが可能になる。

- 降水システム内部にどのような発達段階の降水セルが分布しているのかを示すことにより、降水システムの構造をより正しく理解できると考えられる。